
# INVESTIGATION OF THE EFFECT OF CR ADDITION ON THE MECHANICAL AND MACHINABILITY PROPERTIES OF CR-MO STEELS PRODUCED BY POWDER METALLURGY

**2022**
**MASTER THESIS**
**BIOMEDICAL ENGINEERING**

**Abdul Rahman VASSOUF**

**Thesis Advisors**

**Assoc.Prof.Dr. Mehmet Akif ERDEN**
**Assist.Prof.Dr. Mahir AKGÜN**

# INVESTIGATION OF THE EFFECT OF CR ADDITION ON THE MECHANICAL AND MACHINABILITY PROPERTIES OF CR-MO STEELS PRODUCED BY POWDER METALLURGY

**Abdul Rahman VASSOUF**

**T.C.**
**Karabuk University**
**Institute of Graduate Programs**
**Department of Biomedical Engineering**
**Prepared as**
**Master Thesis**

**Assoc.Prof.Dr. Mehmet Akif ERDEN**
**Assist.Prof.Dr. Mahir AKGÜN**

**KARABUK**
**June 2022**

I certify that in my opinion the thesis submitted by Abdul Rahman VASSOUF titled "INVESTIGATION OF THE EFFECT OF CR ADDITION ON THE MECHANICAL AND MACHINABILITY PROPERTIES OF CR-MO STEELS PRODUCED BY POWDER METALLURGY" is fully adequate in scope and in quality as a thesis for the degree of Master of Science.

Assoc.Prof.Dr. Mehmet Akif ERDEN .....
Thesis Advisor, Department of Biomedical Engineering

Assist.Prof.Dr. Mahir AKGÜN Online
Thesis Advisor, Department of Machinery and Metal Technologies

This thesis is accepted by the examining committee with a unanimous vote in the Department of Biomedical Engineering as a Master of Science thesis. June 24, 2022

| Examining Committee Members (Institutions) | Signature |
|---|---|
| Chairman : Assist.Prof.Dr. Muhammed ELİTAŞ (BŞEU) | Online |
| Member : Assoc.Prof.Dr. Mehmet Akif ERDEN (KBU) | ..... |
| Member : Assist.Prof.Dr. Yasin AKGÜL (KBU) | ..... |

The degree of Master of Science by the thesis submitted is approved by the Administrative Board of the Institute of Graduate Programs, Karabuk University.

Prof. Dr. Hasan SOLMAZ .....
Director of the Institute of Graduate Programs

*"I declare that all the information within this thesis has been gathered and presented in accordance with academic regulations and ethical principles and I have according to the requirements of these regulations and principles cited all those which do not originate in this work as well."*

Abdul Rahman VASSOUF

## ABSTRACT

**M. Sc. Thesis**

**INVESTIGATION OF THE EFFECT OF CR ADDITION ON THE MECHANICAL AND MACHINABILITY PROPERTIES OF CR-MO STEELS PRODUCED BY POWDER METALLURGY**

**Abdul Rahman VASSOUF**

**Karabük University**
**Institute of Graduate Programs**
**The Department of Biomedical Engineering**

**Thesis Advisor:**
**Assoc. Prof. Dr. Mehmet Akif ERDEN**
**Assist. Prof. Dr. Mahir AKGÜN**
**June 2022, 80 pages**

By using powder metallurgy (PM) techniques, materials with complex particle geometry can be produced with a relative lower cost compared to conventional steel production methods such as casting. In addition, the PM methods allow accurate preparation of various alloy compositions.

The amount and type of alloying elements included in the steel composite play an important role in determining the mechanical and structural properties of steel, as they affect hardness, yield, strength and tensile strength. Thus, it directly affects the machinability. In powder metallurgy (PM), molybdenum, nickel, and copper are the most common alloying elements, because they are less sensitive to oxidation during sintering process. However, recently some studies on the oxidation of chromium

during sintering process show that materials based on Cr-alloyed powders are less sensitive to sintering atmosphere compared to materials made from powder mixed with high chrome additives.

Because of the good mechanical properties that result from the use of chromium as an alloying element, this has attracted the interest of some scientists and researchers in the field of biometals because this type of steel composites can be used in some biomedical applications.

In this thesis work, chromium was added to Fe-Mo metal matrix composite (MMC) in different proportions, and an MMC was produced using PM method. In the production process, the powders were mixed with a three-axis (triaxial) mixer for about couple of hours while pressed at high pressing pressure, and then sintered at high temperature.

The microstructures and surfaces of the steel samples produced were examined using an optical microscope and a scanning electron microscope (SEM). Density measurements were performed and porosity amounts were calculated. Tensile tests, corrosion tests and machinability tests were applied.

After reviewing the results of mechanical and structural tests, the possibility of using Chromoly steels manufactured using powder metallurgy in biomedical applications was discussed.

**Key Words :** Powder metallurgy, chrome alloyed steel, metal matrix composite, biometals, chromium effect.

**Science Code :** 92503

# ÖZET

**Yüksek Lisans Tezi**

## TOZ METALÜRJİSİ İLE ÜRETİLEN CR-MO ÇELİKLERİNE CR İLAVESİNİN MEKANİK VE İŞLENEBİLİRLİLİK ÖZELLİKLERİNE ETKİSİNİN ARAŞTIRILMASI

**Abdul Rahman VASSOUF**

**Karabük Üniversitesi**
**Lisansüstü Eğitim Enstitüsü**
**Biyomedikal Mühendisliği Anabilim Dalı**

**Tez Danışmanı:**
**Doç. Dr. Mehmet Akif ERDEN**
**Dr. Öğr. Üyesi Mahir AKGÜN**
**Haziran 2022, 80 sayfa**

Toz metalurjisi (TM) teknikleri kullanılarak, döküm gibi geleneksel çelik üretim yöntemlerine kıyasla karmaşık parçacık geometrisine sahip malzemeler daha düşük maliyetle üretilebilmektedir. Ek olarak, TM yöntemleri, istenilen çeşitli alaşım bileşenlerinin yüksek hassasiyette hazırlanmasına imkân vermektedir.

Çelik kompozitte bulunan alaşım elementlerinin miktarı ve türü, sertlik, akma, mukavemet ve çekme mukavemetini etkilediğinden çeliğin mekanik özelliklerinin belirlenmesinde önemli rol oynar ve bundan dolayı işlenebilirliğini etkiler. Toz metalurjisinde, molibden, nikel ve bakır, sinterleme işlemi sırasında oksidasyona daha az duyarlı oldukları için en yaygın alaşım elementleridir. Ancak son zamanlarda sinterleme işlemi sırasında kromun oksidasyonu üzerine yapılan bazı çalışmalar, Cr

alaşımlı TM malzemelerin, yüksek krom katkıları ile karıştırılmış tozlardan yapılan malzemelere kıyasla sinterleme atmosferine daha az duyarlı olduğunu göstermektedir.

Kromun bir alaşım elementi olarak kullanılmasından kaynaklanan iyi mekanik özellikler nedeniyle, bu tür çelik kompozitler bazı biyomedikal uygulamalarda kullanılabildiği için biyometaller bazı araştırmacıların ilgisini çekmiştir.

Bu çalışmada, TM yöntemiyle Fe-Mo metal matrisli kompozite (MMK) farklı oranlarda krom eklenmiştir. Üretim sürecinde tozlar, üç eksenli (triaxial) bir karıştırıcı ile yüksek presleme basıncında preslenirken yaklaşık iki saat karıştırılmış ve ardından yüksek sıcaklıkta sinterlenmiştir.

Üretilen çelik numunelerin mikroyapıları ve yüzeyleri optik mikroskop ve taramalı elektron mikroskobu (SEM) kullanılarak incelenmiştir. Yoğunluk ölçümleri ve porozite oranları hesaplanmış, çekme, korozyon ve işlenebilirlilik testleri de uygulanmıştır.

Mekanik ve yapısal testlerin sonuçları incelendikten sonra toz metalurjisi kullanılarak üretilen Kromoly (Chromoly) çeliklerinin biyomedikal uygulamalarda kullanılabilirliği tartışılmıştır.

**Anahtar Kelimeler :** Toz metalurjisi, krom alaşımlı çelik, metal matrisli kompozit, biyometaller, krom etkisi.

**Bilim Kodu** **:** 92503

## ACKNOWLEDGMENT

First of all, I would like to give thanks to my advisors, Assoc. Prof. Dr. Mehmet Akif ERDEN and Assits. Prof. Dr. Mahir AKGÜN, for their great interest and assistance in preparation of this thesis, this thesis would not have been possible without their constant guidance and support.

Special thanks to Scientific Research Projects (BAP) Coordination Unit of Karabük University (Karabük, Turkey) for supporting this work under Project Number: KBÜBAP-21-YL-118.

Finally, I must express my very profound gratitude to my parents whose constant love and support keep me motivated and confident. My accomplishments and success would not have been possible without them. Deepest thanks to my friends, who keep me grounded, remind me of what is important in life, and are always supportive of my adventures.

**CONTENTS**

**Page**

**Page**

**Page**

## LIST OF FIGURES

**Page**

**Page**

## LIST OF TABLES

**Page**

## SYMBOLS AND ABBREVITIONS INDEX

### SYMBOLS

Ni : Nickel

Mo : Molybdenum

V : Vanadium

Mn : Manganese

Cr : Chromium

Fe : Iron

Ti : Titanium

Nb : Niobium

C : Carbon

W : Tungsten

Mg : Magnesium

Co : Cobalt

O : Oxygen

N : Nitrogen

### ABBREVITIONS

PM : Powder Metallurgy

Log : Logarithms

SEM : Scanning Electron Microscope

EDS : Energy Dispersive X-Ray Spectroscopy

XRF : X-Ray Fluorescence

FCC : Face Centered Cubic

EDS : Energy Dispersive X-Ray Spectroscopy

| | |
|---|---|
| AD | : Anno Domini |
| SI | : International System of Units |
| CNC | : Computerized Numerical Control |
| ISO | : International Organization for Standardization |
| S/N | : Signal to Noise ratio |
| SBF | : Simulated Body Fluid |
| PBS | : Phosphate Buffered Saline |
| CI | : Confidence Intervals |
| Ra | : Surface Average Roughness |
| Vb | : Flank Wear |
| ANOVA | : Analysis Of Variance |

# PART 1

## INTRODUCTION

Alloyed steels are steels whose mechanical properties are improved by adding alloying elements such as Mo, V, Mn, Ni and Cr in a in certain proportions. The properties of alloyed steel change according to the shape, size and distribution of the alloyed elements within the metal structure. Therefore, formation conditions are very important in terms of determining the mechanical and structural properties of alloyed steels.

It is more difficult to control these properties in the conventional metal casting methods than in the powder metallurgy (PM) method. Therefore, in this study, it is aimed to investigate how the production of alloy steel alloyed with chromium, molybdenum and graphite in different proportions by powder metallurgy method affects the mechanical properties. The study is also aims to investigate the effect of adding chromium in varying proportions on the general properties of steel.

As it is known, the use of the powder metallurgy method will reduce production costs significantly, the resulting metal has good mechanical properties and high quality surface, and also there will be the ability to produce metals that are difficult to produce using other methods. Thanks to powder metallurgy technology, it will be possible to manufacture small-sized metal parts with high mechanical properties in various industrial fields.

In this study, Mo-Cr steel was produced in different compositions. Tests such as tensile and hardness tests were applied to the produced parts. The ideal sintering conditions and temperature and the mechanical properties of the steel parts manufactured using the powder metallurgy method were determined by performing microstructural tests such as (SEM microstructure, SEM fracture surface, SEM EDS analysis).

After determining the mechanical properties of the samples made using powder metallurgy, a corrosion test was performed on a number of samples in a simulated body fluid (SBF) to study their potential use in medical applications such as medical implants.

# PART 2

# STEELS

## 2.1. STEEL DEFINITION AND CLASSIFICATION

Iron-carbon alloys are examined in two main groups as "Steels" and "Cast Irons" according to the carbon ratio they contain. According to this classification, alloys that contain less than 2% carbon are called steel while alloys with more than 2% carbon are called cast iron [1]. Steels are classified into several different classes based on: usage areas, chemical composition, applied heat treatment, shaping method, microstructure and production method. It is important to discuss alloying elements due to their importance in the steel production process, as they cause changes in terms of mechanical and thermal properties of the resulting steel. When we classify steels in terms of chemical composition, it is divided into "Alloy steel" and "Non-alloy steel".

One of the chemical properties of steel is that it is suitable for welding processes. It is harder and stronger than iron. When heat treatment is applied, mechanical, electrical and physical properties can be gained and enhanced. With different processes, steel's hardness and strength can increase at high temperatures. It can be shaped by pressing, forging and rolling methods applied within a certain temperature. Some steels with specific properties have the ability to be formed when they are cold. Metals can be coated with plastic compounds [2,3].

When a hot steel is quenched (dipped in water) suddenly and rapidly, it shows changes in its crystalline properties, with increase in the hardness. This process is called "steel quenching" [4]. Stainless steels are heat and corrosion resistant, fully recyclable, and easy to be cleaned and manufactured. Alloy steels containing high carbon ratio are called "Cast iron". As the carbon ratio increases, the tensile and yield strength of the steel increases, while reducing its formability and welding capabilities [5].

An alloy made of carbon and iron is called steel, the term "alloy steel" is used to express that the steel composition contains alloying elements other than carbon. Essentially, Carbon is like other alloying elements, it acts as an alloying element in the structure of the steel [6].

### 2.1.1. Alloy Steels

While iron and carbon alloys contain only iron and carbon, alloy steels contain other alloying elements such as chromium, manganese, silicon, nickel and molybdenum in addition to iron and carbon. In addition, alloyed steels are classified into: low alloyed and high alloyed steels according to the ratio of alloying elements. Low-alloyed steels containing less than 5% alloying elements, they are usually used in the production of machine parts and high-strength structural elements.

One of the changes caused by alloying elements is the transformation temperatures in the iron-carbon thermal equilibrium diagram. Since almost all of the elements are austenite at room temperature, it affects face-centered cubic (FCC) crystals. Elements that dissolve in each other form the face-centered cubic (FCC) structure. Thus, the alloying elements transform from the gamma phase to the ferrite phase in the opposite direction. Alloying elements fix the austenite and expand the available temperature range.

High alloy steels are steels contain alloying elements ratio greater than 5%. When Non-alloyed and low-alloyed steels do not contain the desired properties or have insufficient properties, high-alloyed steels are preferred. Stainless steels and steels used in tools manufacturing can be given as examples [7].

Low alloy steels have basically similar behavior to unalloyed (Non-alloy) steels and the most important feature is their superior hardenability. The deficiency in the use of unalloyed steels is that because low alloy steels is more preferred are as follows. The impact resistance of unalloyed steels is very low at low temperatures, the depth of hardness formed by quenching, and the oxidation and corrosion resistance of unalloyed steels are low [8,9]. Based on these disadvantages of unalloyed steels, steels that are

produced and contain manganese, nickel, chromium, molybdenum, and tungsten as basic alloying elements in the mixture (low alloy steels) are more common to use. In addition, alloying elements such as aluminum, vanadium, boron, niobium, titanium, lead, copper and cobalt also can be added to these steels.

### 2.1.2. Non-Alloy Steels (Carbon Steals)

Non-Alloy steel is a type of steel that, contains only carbon as alloying element, but can also contain elements at the level of 1.65% manganese, 0.6% silicon and 0.6% copper in its composition. In another nomenclature, it is called "plain carbon steel" [10].

In non-alloy steels carbon is the most valuable alloying element. Therefore, steels are categorized according to the carbon ratio they contain, as "Low Carbon Steels", "Medium Carbon Steels" and "High Carbon Steels" [10].

At high temperatures, the material softens and its yield limits decrease, and it is exposed to plastic deformation at low stresses. Permanent deformations that occur slowly in long-term stresses cause the material to break after a certain period of time [11].

## 2.2. DEVELOPMENT OF STEELS

Steel is an alloy that started to be used since early time of human history and still continues today. Although it was known in ancient times, the use of steel was limited to weapons and similar war materials, since it was not commonly used in construction, industrial and development applications. With the development of technology in the last few centuries, raw iron production started in England exactly in the 18th century. After this stage of history, steel and iron structures have started to be made in the world. We can say that the first steel structures were bridges [12].

One of the most important structures built using steel and iron is the Eiffel Tower. The tower, which was finalized in 1889, is a good example of the steel usage over the years.

Steel is considered as one of the most important materials needed and used in engineering applications. In particular, it can be said that the period after World War II was the beginning of an acceleration in the development of steel production. The need for steel in many sectors is increasing day by day. With the increasing strength to weight ratio resulting from the development of lighter and thinner steels. Steel production and manufacturing costs have been reduced [13–22].

## 2.3. STEEL STRENGTH INCREASING MECHANISMS

The mechanical properties of materials are highly dependent on the behavior of their metallurgical structures. Since the metallurgical structure changes with the thermal and mechanical processes applied to the material together with the chemical composition, it can be said that the mechanical properties of the material also depend on these conditions. One of the most important material properties is the strength. Other properties are vary depending on strength. In materials science, the resistance can be explained as the material's resistance against plastic deformation. Plastic deformation of metals is formed by the progression of linear defects. Therefore, mechanical properties such as hardness, ductility, and strength explain the density of dislocations in the internal structure of metals and their interaction with other defects [7]. Strength enhancing processes can be listed as follows.

- Precipitation Hardening (Aging).
- Hardening by Reducing Grain Size.
- Cold Process.
- Alloy Hardening.
- Hardening by Martensitic Transformation.
- Deformation Aging.
- Hardening by Dispersion.

It is necessary to know the mechanical properties-microstructure relations in detail in order to improve some of the desired properties in microalloyed steels and to make the most of the improved steels. Hardening mechanisms such as grain size hardening, solid

melt hardening, precipitation hardening, strain hardening and hardening mechanisms used in microalloy steels increase the strength of the steels. While the grain reduction mechanism increases the strength in mentioned hardening mechanisms, it also improves the toughness [23].

## 2.4. ADVANTAGES AND DISADVANTAGES OF ALLOY STEELS

Compared to plain carbon steels, alloy steels have superior hardness, strength, wear resistance, toughness, hardenability and hot hardness. In order to gain these advantages, heat treatment may be required. Alloy steel has high strength. The ratio of its own weight to the load it carries is very small, so the overall weight of the structures decreases [7].

Strong carbide-forming elements such as Ti, Nb and V form carbide. Alloying elements also affect the eutectoid temperature. (i.e. Mn and Ni reduce eutectoid temperature). That's why they are known as austenite builders. Carbide-forming elements raise the eutectoid temperature and are known as ferrite-formers. Alloy steel is more costly than unalloyed steels [7].

## 2.5. ALLOY STEELS USES

Alloy steel is a valuable alloy that contributes to a large part of our lives, from the construction sector to the healthcare field, and the materials used to the technological industries, steel is used in the production of products such as communication equipment, automotive industry, steam boilers, aviation industry, dairy equipment, leather, chemical and petroleum industry, paper and soap industry, small household appliances, nuclear engineering, exhaust production decorative pipes, heat-resistant parts and containers.

Stainless steels, which doesn’t cause chemical changes in the human body and the foods are used the manufacture of medical devices and food preservation equipment, also they are used in the medical sector such as hips and knee caps, screws, prostheses, needles and scalpels. Stainless steel plates, which do not spoil the characteristics of the

food such as color and smell, are safely preferred in storage containers produced for food and beverages, oven molds and coated pots.

## 2.6. ALLOYING ELEMENTS

Alloying elements play an important role in performing thermomechanical processes. While Mn, Mo, and Cr elements are effective especially due to their hardening, there are different mechanisms in Nb, V and Ti microalloying elements. They extend the toughness and increase strength by hardening and grain refinement method. However, grain refinement contributes to the increase of toughness and strength at the same time [24].

The alloy that contains 0.2%-2.1% carbon (C) in its composition and is formed by the effect of the carbon-iron (Fe) mixture is called steel. A few of other elements that make up this alloy are nickel (Ni), molybdenum (Mo), cobalt (Co), tungsten (W), magnesium (Mg), manganese (Mn), vanadium (V) and chromium (Cr). When these elements are included in the metal composite, the steel turns into a stainless form or becomes harder [7].

### 2.6.1. Carbon and Graphite

Carbon (C) is located in the sixth row of the periodic table, carbon can be found in different formations in nature. The atomic number of carbon is 6. It has hexagonal or cubic crystal structure, carbon can be black or gray in color. The branch of science that studies carbon and its components is called organic chemistry [25].

The high carbon ratio causes an increase in the perlite structures and a decrease in weldability and toughness. However, it also increases the yield strength. In addition, the use of carbon at high rates causes bainitic and martensite structures to be prominent. The maximum use of carbon in microalloyed steels is 0.2% under hot rolling conditions. However, since the forged parts, which are frequently used in the automotive industry, are produced only with the controlled cooling mechanism method, the carbon ratio is above 0.25% [26].

The term "graphite" is derived from the Greek word "Graphein", which means writing. The usage areas of graphite material started long time ago. The first pencil production from graphite material was carried out in England in the 15th century. By the 18th century, it was found that the graphite is one of carbon allotropes [27,28].

In terms of thermodynamics, it was seen that graphite has a more stable structure than carbon at atmospheric pressure. Above 1500 °C, diamond turns into graphite [29].

Graphite, which is known to be one of the softest materials, is a different formation of carbon and is especially used for lubrication process. Graphite can be found in nature in a natural form. However, it can be obtained by processing petroleum coke in oxygen-free furnaces. Graphite is found in nature in Alpha and Beta forms. Alpha and Beta graphite have the same physical features. But they have different crystal structures. Artificially manufactured graphite is known as Alpha type graphite. Besides its use as a lubricant, it is widely used in steel production. Carbon has two allotropes in its atomic arrangement, graphite and diamond [29].

Graphite is a material with good thermal conductivity and electrical properties. It also has the ability to maintain its form at high temperatures. It shows its refractory properties well at high temperatures. Graphite is a functional material that has been used in many applications that benefit humanity since its discovery [30].

Although artificially-made graphite applications are still one of great interests today, natural graphite is preferred in some applications. Natural graphite has three different types: crystalline (vein), amorphous and granular (flake). These names were chosen because they give information about their forms [25].

The evolution of graphite production started with the interest in carbon production technologies in the 19th century. Synthetic graphite, which is created to be used in industrial furnaces as an electrical resistance material, reveals rapid developments in the next stages. In the production of special form graphite, graphitization processes of carbon materials are obtained by applying heat treatment method at 2600-3300°C. In the graphitization process, the carbon clusters turn into three-dimensional graphite.

Graphite materials with different crystalline structures are obtained based on additives, raw materials and processing parameters [31]. The distances between dislocations and the crystal structure of graphite change with temperature. The distance between these layers decreases as the heat treatment temperature rises.

Generally carbon is the alloying element of iron. Sometimes, different elements such as Chromium, manganese and Magnesium can be used as an alloying element. Changing the percentage of alloying elements in the steel composite cause changes in terms of ductility, hardness and stress point. Steels with a high carbon content are stronger and harder than iron, but less ductile [10].

### 2.6.2. Molybdenum

Molybdenum is an alloying element with carbide and ferrite-forming properties. When molybdenum is added to the steel composite -even in small ration- the result is a high-strength steel that has a high structural stability when placed under high pressures reaching to 210,000,000 $kg/m^2$. Theses massive levels of strength have high thermal properties, making molybdenum steels suitable for use in the missile and aircraft industries [7,10].

When molybdenum is present in low alloy steels at a ratio of about 0.15-0.30% together with Ni, it increases the hardenability of the steel, the resistance to the drawing process and heat. In addition, it enhances the wear resistance [32].

Molybdenum obtained by acid-base reactions cannot be found in nature. It includes features such as high wear resistance, temperature resistance, and low coefficient of friction. It has a melting temperature of 2610°C and a density of 10.22 $g/cm^3$, it is highly sensitive to impurities at the grain boundaries. It may show intergranular fracture even in completely recrystallized medium. Molybdenum is used in many applications such as: steel alloying, dentistry, electronics, aircraft and spacecraft construction, nuclear energy applications. Since molybdenum oxidize above 500°C, it is necessary to protect the Molybdenum by covering it with an anti-oxidation layer while working in such environment. Molybdenum transforms into $MoO_3$ at the

temperature of 700°C in atmospheres containing oxygen. This oxide has the shape of a white odorless smoke. Because of evaporation, a protective oxide layer cannot be formed on the surface of Molybdenum and the metal keeps losing its weight continuously [33].

### 2.6.3. Chromium

Chromium is considered one of the elements that positively affects the hardenability of steel. Due to this positive effect, if manganese is added to steels containing 5% or more chromium, the critical quenching rate is seriously reduced, and the steel can be hardened in air without the need to use water or oil. In addition, since chromium is a strong carbide former, it positively affects the hardness and wear resistance of the steel. Another well-known important effect of chromium is that it makes steels resistant to corrosion. So much so that steels containing 14% or more chromium are classified as stainless steel. Although chromium is preferred because it increases the tensile and high temperature strength of steels, it can also create negative effects such as reducing ductility or causing temper brittleness. In order to reduce these negative effects, we see that chromium is often used together with nickel and molybdenum [34].

### 2.6.4. Nickel

Nickel is the second most used element in powder metallurgy. Nickel causes shrinkage in particle sizes during sintering process, it behaves differently from copper and forms a solid melt with iron at high temperatures [35].

Nickel has a grain reduction effect, it increases and enhances the strength and toughness of the material. When nickel is used with chromium, it increases the ductility, hardness and high fatigue resistance of the alloy. It also reduces the critical cool down rate [36].

Nickel maintains its strength at high temperatures, and its toughness and ductility at temperatures below zero. So it can be easily processed both hot and cold. Therefore, it is easy to machine and weld. Chemically, nickel is non-reactive, insoluble in ammonia

and water. Also, it is unaffected by alkalis and concentrated nitric acid. It dissolves in hydrochloric, diluted nitric, and sulfuric acids [37].

Nickel, has been in use for over 200 years in various applications such as rechargeable batteries, coins, special alloys, magnets, valuables, surgical cables and others. Stainless steels containing 7% Nickel are used in the oil, gas, power industry, marine applications and the chemical industry. Kitchen materials used in homes, are one of the most common uses of nickel steels. In the previous uses, nickel has an intense use due to its strength, high ductility, electrical and thermal conductivity and corrosion resistance properties [38].

## 2.7. MEDICAL IMPLANT CORROSION

To this day, implants in the human body still suffer from Corrosion. It has been well established that it causes the release of metal ions (debris) that are not biocompatible and lead to implant failure [39]. Corrosion has been a persistent problem with medical implants. For example, It has been determined that approximately 41% of the failures of Ti-6Al-4V and 316L implants happened due to corrosion [40,41]. Therefore, it is of great importance to understand the corrosion of all implants used in the human body, and especially orthopedic implants [42].

### 2.7.1. Corrosion

Corrosion is defined as the degradation of metal with the effect of corrosive and aggressive environments. In other words, corrosion is an undesirable chemical reaction of the metal to the environment [42]. Corrosion in the human body occurs gradually. With the placement of orthopedic implants in the patient's body, they come face to face with a very aggressive environment. At the implant/tissue interface inside the human body, various ions such as dissolved oxygen in water, proteins, metal ions ($Na^{+}$, $K^{+}$, $Ca^{+2}$, $Mg^{+2}$), chloride and hydroxide are present [40,41]. Therefore, the corrosion resistance of the metallic implant material is an important factor of biocompatibility. Oxides are the lowest free energy states of many metals in oxygenated and hydrated environments such as the body environment. Corrosion occurs when atoms of the

metal are ionized. Metal ions diffuse into the surrounding environment and combine with ions and components in that environment. For implants, the human body is considered a very aggressive environment in terms of corrosion, because it is not only watery but also contains chloride ions, proteins and different ions [42].

#### 2.7.1.1. Corrosion Types of Medical Implants

Corrosion occurs generally or locally. In general corrosion, the metal surface is known to dissolve uniformly. On the other hand, local corrosion takes place in specific areas on the metal surface. The most relevant corrosion types for metallic alloys used in medical implants are galvanic corrosion, pitting corrosion, crevice corrosion and mechanically assisted corrosion, and these types of corrosion are considered local corrosion [42].

**Galvanic Corrosion**

When any pure metal or alloy is placed in a corrosive and aggressive environment, its electrode potential will be formed as Ecorr. Ecorr is the point at which the rates of oxidation and reduction are exactly equal. Galvanic corrosion is the electrochemical potential difference between two different metals. Theoretically, when two different metals are used, one will be the anode (the one with the lower electrode potential), the other the cathode, and corrosion will start quickly between the two. The galvanic series is an ordered list of experimentally measured corrosion potentials for both pure metals and alloys in natural seawater, as shown in Figure 2.1. When measuring corrosion potentials, the standard electrode can be Standard Hydrogen Electrode (SHE) or Saturated calomel electrode (SCE) [43].

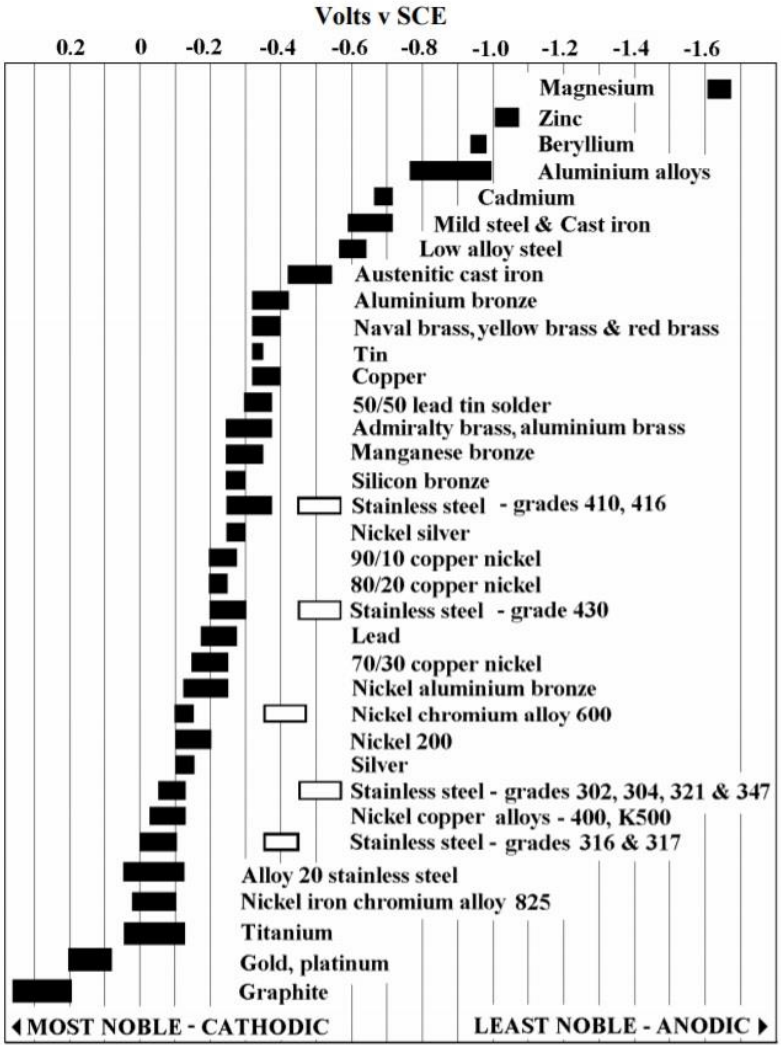


Figure 2.1. Galvanic series in sea water [44].

The galvanic series found experimentally in natural sea water is used to study the corrosion behavior of metallic orthopedic implants used in the human body [20]. Body fluids and Simulated Body fluids (SBF) such as Ringer's solution can be thought of as a diluted version of seawater [43,45].

The type of pure metal or alloy, the composition of the electrolyte, the oxide film layer, and the number of metals or alloys in the electrolyte directly affect the electrode potential [43]. Galvanic corrosion is a huge concern in orthopedic implants because different metals are often used in orthopedic implants.

**Friction Corrosion**

Tribocorrosion is a general term used to describe wear-assisted corrosion. Technically, friction corrosion is a subcategory of tribocorrosion. Friction corrosion is a type of corrosion promoted by micro-movement induced wear. As is known, when a metal is exposed to an aqueous or humid environment, an oxide film forms on it. This layer tries to protect the metal from corrosion. Micro-wear debris disrupts the oxide film on the implant, altering the electrochemical balance and the implant will corrode again. Corrosion will continue until new oxide film is formed. This cycle (debris due to micro-abrasion, deterioration of the oxide film, changing the balance in the environment and formation of a new oxide film) usually occurs in orthopedic joints such as hip implants [42,46].

In the body environment, many parameters affect friction corrosion: oxygen, proteins present, wear, loads applied to the implant, and integration with bone cells. These factors vary in different parts of the body [42].

**Crevice Corrosion**

The first and most fundamental stage of corrosion is the oxidation of the metal. Corrosion ions emerging as a result of this step form an oxide film on the metal. The main purpose of this oxide film is to protect the metal from further corrosion [40]. In addition, the thickness and composition of the oxide film varies depending on the type of metal and its reactions with living tissues. Even low concentration of dissolved oxygen, inorganic ions, proteins and cells can accelerate the release of metal ions. The regeneration time after the degradation of the surface oxide film also decides the amount of ions released. Most of the time, these deteriorations occur due to crevice or pitting corrosion [40,47,48].

Crevice corrosion:

- It is caused by small galvanic cells on the surface of the implant due to its inhomogeneity, which causes cracks when the material is eroded.

- It occurs in fatigue cracks and other cracks where the effect of oxygen is reduced.

- Occurs in areas where oxygen is not available in abundance. For example, crevice corrosion that occurs in geometric spaces such as the modular interfaces of hip implants [42].

At the beginning of crevice corrosion, oxygen reduction occurs both on the surface of the implant exposed to the electrolyte and on the part inside the crack. However, the external metallic part of the implant exposed to the electrolyte supplies abundant oxygen from the environment, maintaining the concentration of $O_2$ in a steady state. On the contrary, in the crack, the level of $O_2$ decreases because there is no circulation of oxygen. The difference in the concentration of $O_2$ inside and outside the crack makes the metal part exposed to low oxygen concentration the anode and the external metal part the cathode. The electrode potential difference between the inner and outer metal will initiate corrosion of the cracked metals [42,49].

The onset of crevice corrosion largely depends on the geometry of the crack. Narrow cracks initiate crevice corrosion more rapidly. Because in such cracks, diffusion of oxygen amount, which will protect the passivity of the oxide film, is prevented [42,49].

**Pitting Corrosion**

Pitting corrosion is a local corrosion attack triggered by the presence of aggressive anions. This type of corrosion causes significant release of metal ions and damage to implants [47]. Pitting refers to the formation of small holes on the surface of an implant protected by a thin oxide film [49]. The sites where these pits occur are typically associated with a site of crevice corrosion or are at modular conical joints. Pitting corrosion is associated with many factors such as pH, surface temperature, presence of coating, state of the material and components of the alloy. These factors determine the properties of the oxide film on the implant. Pitting corrosion, stress corrosion cracking or fatigue cracks that can disrupt the implant can allow it to occur [42,50]. Pitting corrosion creates a small anodic zone above the implant. The ruptures that may

occur in the anodic region oxide film are caused by different components used in the alloy of the implant, surface irregularities and missing coatings [49]. The movement of metal and hydrogen ions from the bottom of the pit into the solution is restricted by the film covering the top of the pit. Due to the depletion of oxygen, there is a difference in the electrochemical potential between the pit and the surrounding metal surfaces. As a result, corrosion will be triggered quickly [42,49]. Pitting corrosion is shown in Figure 2.2.

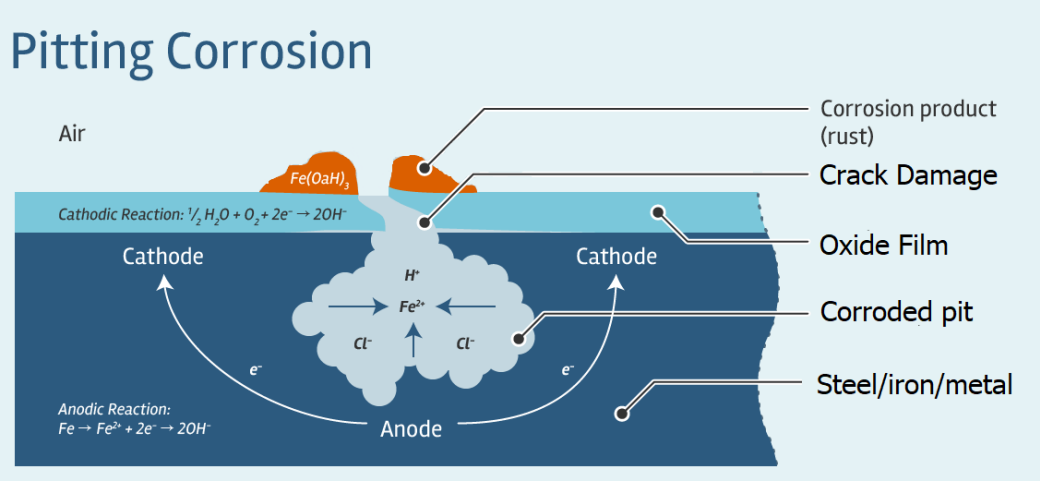


Figure 2.2. Pitting corrosion [51].

## PART 3

## POWDER METALLURGY

Powder metallurgy (PM) is a process of creating metal parts by raising the temperature of metal powders to reach temperatures below their melting points. In other words, powder metallurgy is a metal shaping method that forms near-net parts from metal powders. PM extends to the action of mixing unalloyed or alloyed powders using specific proportions, compressing the homogeneously mixed powders with the help of a suitable mold, and then sintering the powders in a controlled atmosphere in order to gain their metallurgical properties. The production of homogeneous parts ensures that their physical, chemical and mechanical properties can be controlled [52].

The process of powder metallurgy has played an important role in human history for thousands of years. The history of the powder mining process goes back to a very ancient time. For example, the ancient Egyptians obtained sponge iron by using iron oxide, in the years after 400 AD, the iron pillar of Delhi weighing more than 3 tons was built in India using powder metallurgy resembling methods used today. Coming to the 1826, the first application of powder metallurgy was in Russia when platinum coins were produced. In 1892, W.H. Wolaston was the first person who started the first official powder metallurgy application by obtaining platinum using powder metallurgy method.

Hot and cold pressing in powder metallurgy have been greatly developed to replace traditional casting processes in many applications. In the period after World War II, powder metallurgy was included in the scientific literature as a new method for metal production.

8000 alloys have emerged using 86 elements in the periodic table, which are considered metals. It is possible to produce about 1025 alloys from the 86 elements

Mentioned, with different mixtures such as binary, triple and quaternary. The only method that can make this possible is the powder metallurgy method [7].

Considering the present day, the powder metallurgy method is a very valuable method because it gives a product of high quality and excellent properties at a relatively low cost compared to the traditional methods. The parts planned to be produced by powder metallurgy method will have the feature of being used immediately after they are produced, or they can be left for secondary processes upon request. The production of materials that cannot be produced with the classical production and casting method can be realized with the powder metallurgy method [53], Figure 3.1 shows powder metallurgy stages.

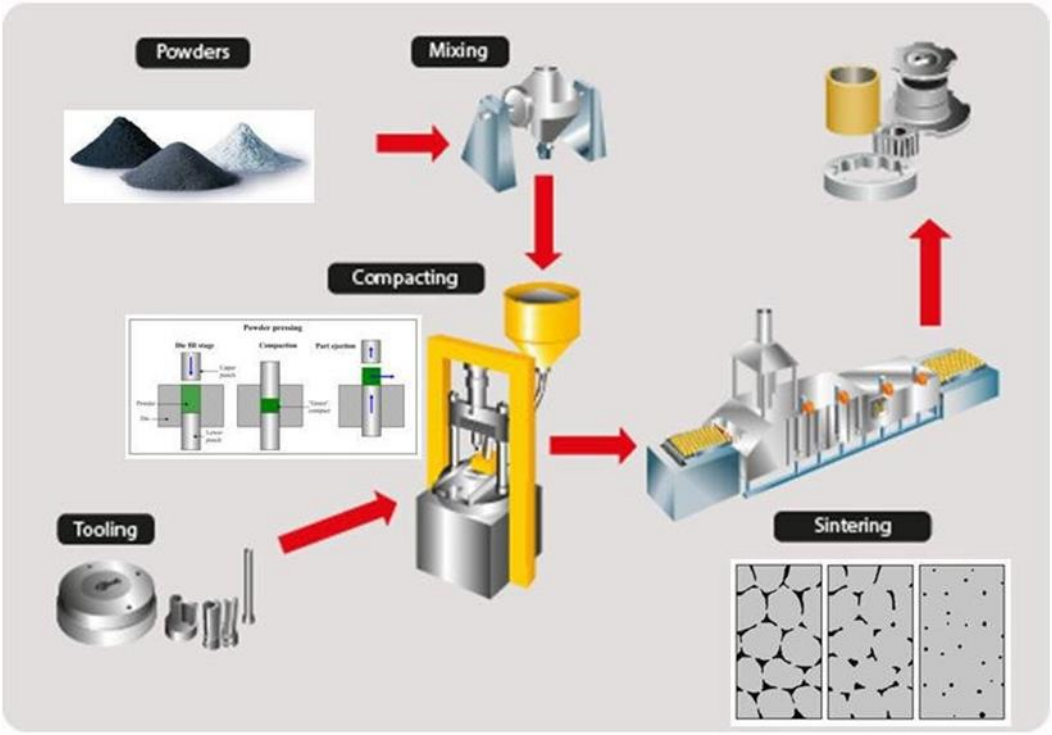


Figure 3.1. Powder metallurgy stages [54].

### 3.1. POWDER PRODUCTION

The methods used in the production of metal powders are responsible for determining many properties of the metal powders. The geometric form of the powder can vary greatly, from complex shape to spherical shape, depending on the used production

method. The surface state of the powder particle also differ according to the used production method. Many of the materials can be pulverized by a technique suited to their properties. The following are the techniques used in the production of metal powders [55]:

- Solid State Reduction.
- Atomization.
- Electrolysis.
- Chemical reduction.
- Mechanical (Grinding).
- Other production techniques.

### 3.1.1. Solid State Reduction

In solid-state reduction, the metal ore is smashed and crushed, usually mixed with carbon, and processed using a continuous furnace. In the furnace, a chemical reaction occurs, reducing the oxygen and carbon from the powder that leaves a cake of sponge metal which is being crushed after that, separated from all non-metallic material, and sieved to form powder. As no refining operation is involved in the production process, the purity of the powder depends entirely on the purity of the raw materials used. The non-uniform and irregular sponge-like particles are soft, easily compressible, and give compacts of good pre-sinter strength (green strength) [56].

### 3.1.2. Atomization

Atomization, is a method that can be used in powder production of all molten metals. In this process, molten metal is divided into small tiny droplets and frozen quickly before the droplets come into contact with a solid surface or with each other. Generally, a thin flow of molten metal is crumbled by subjecting it to the impact of high-energy jets of liquid or gas as shown in Figure 3.2. In principle, this technique can be applied and used with all metals that can be smelted and it is used in the production of brass, alloy steels, bronze, iron, copper, metals with low-melting-point such as lead, zinc, tin, cadmium and aluminum [56].

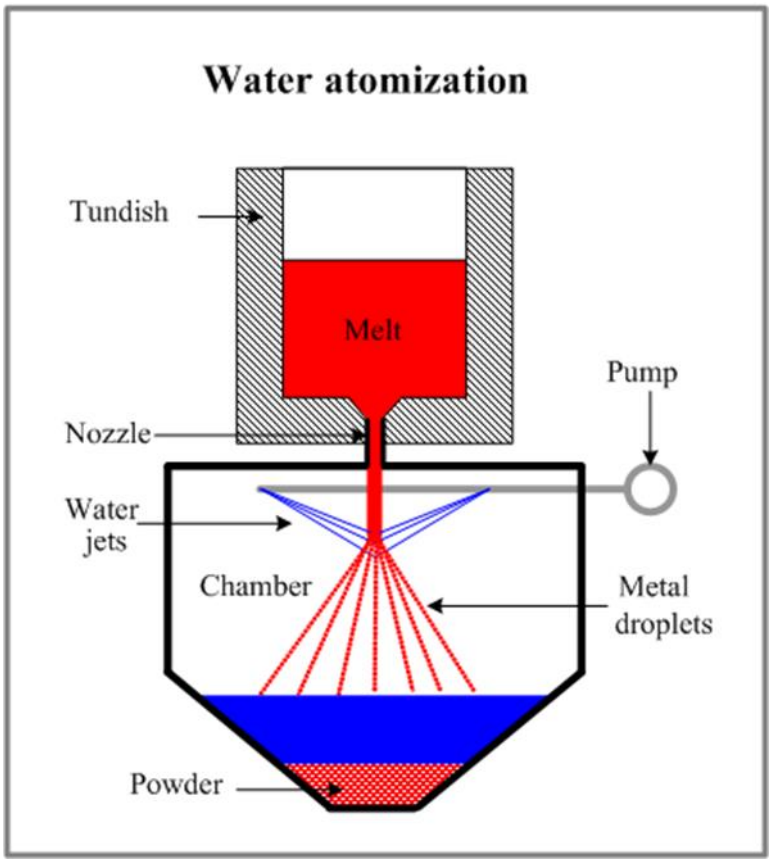


Figure 3.2. Water atomization process [57].

Since all the metals that make up the alloy are alloyed in the molten position, it is a useful to produce the alloys as powder particles. Thus, the powder particles will have a one-to-one chemical composition. One of the advantages of the atomization method that it can be used easily in melting alloy powders, all the grains in the amount of powder are identical [7]. Below are some of the techniques used in the atomization process:

- Gas atomization technique.
- Water atomization technique.
- Vacuum atomization technique.
- Centrifugal atomization.

More than 75% of metal powders produced are produced using the atomization technique. Atomization techniques can be used to produce powders from all fusible

metals and alloys. 80% of the powder particles produced by the atomization technique are produced by the water atomization technique [58].

### 3.1.3. Electrolysis

By choosing the proper conditions such as chemical composition, current density and the temperature of the electrolysis, many powders or metal sponges can be deposited on the cathode. The next stages are washing, drying, reducing, annealing and grinding. Copper, chromium and magnesium metal can be formed using this method. Electrolytic powders have high purity [59].

### 3.1.4. Chemical Reduction

Chemical reduction is a common method used in the production of iron powders. The metal ore selected by this method is crushed, then mixed with coke, then the composite is passed through a continuous furnace where reduction occurs (Continuous furnace is shown in Figure 3.3), and sponge iron is produced in a cake form. After that, sponge iron is grounded, separated from non-metallic materials before being sieved. The result materials depend on the purity of the powders. Particles in irregular spongy form are smooth and soft. They can be simply compressed, the result samples have good strength. Similarly, refractory metals are obtained by reduction of their oxides with hydrogen [60].

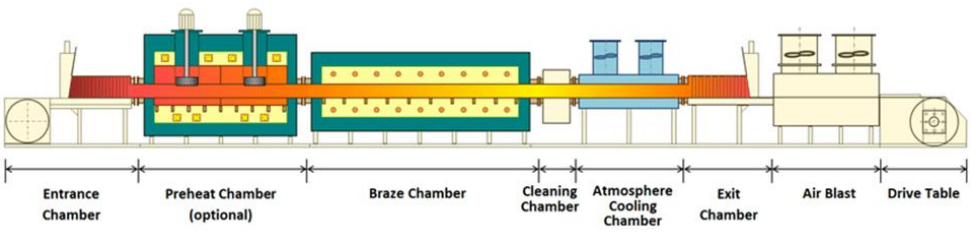


Figure 3.3. Continuous furnace [61].

### 3.1.5. Grinding Method

Grinding is a mechanical process mostly done in ball mills. Using this technique brittle material powders are produced, the basic principle is to ensure that an impact occurs between a hard object and the material to be crushed. The metal to be grinded is placed in a container containing large-diameter hard and wear-resistant balls. The material to be ground is divided into very small powders with large-diameter then added to the grinding container such as shown in Figure 3.4. If the milled material is brittle, it will be broken into very small powders by the impact of the balls. If the milled material consists of ductile particles, they become flattened by deformation as a result of collision. For a homogeneous mixture, the volume of the balls to be placed in the container and the amount of material to be grinded are very important. The volume of the balls should be approximately half of the container volume and the amount of material to be grinded should be approximately 25% of the container volume. Brittle materials such as iron-chromium, iron alloys, and iron-silicon are mechanically ground in ball mills [62].

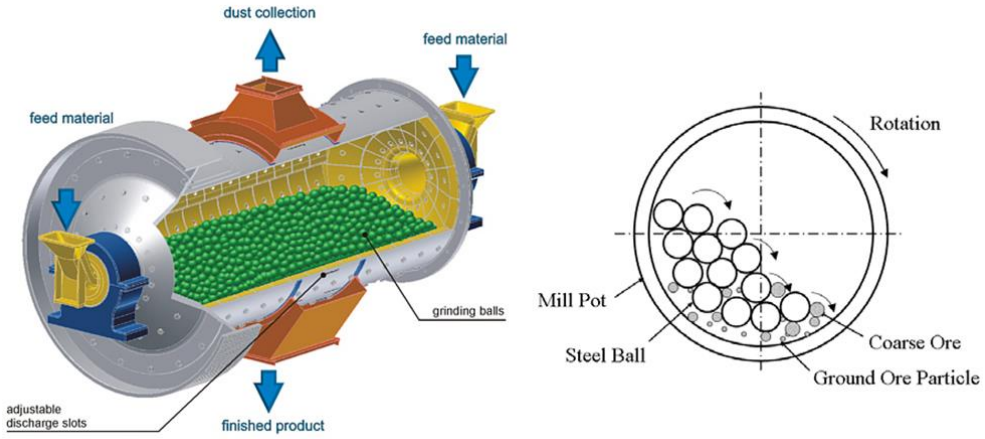


Figure 3.4. Grinding process [63,64].

## 3.2. ADVANTAGES AND DISADVANTAGES OF POWDER METALLURGY

Powder metallurgy method, is like other methods, has its pros and cons. In this section, the most important advantages and disadvantages of powder mining compared to other methods will be reviewed.

### 3.2.1. Advantages

- The materials produced have high mechanical and physical properties.
- Materials with different characteristics that do not dissolve in each other can be produced by combining them.
- The particle size of the produced parts is small, the tensile strength and machinability are high.
- Parts produced with powder metallurgy generally do not require additional processes such as machining.
- There are no melting losses.
- Materials with high wear resistance and high hardness can be produced.
- After the sintering process, the part is ready for use and there is no need for secondary operations.
- It can be easily produced in parts with complex forms and precision.

### 3.2.2. Disadvantages

- The cost of metal powder particles is more expensive than materials used in casting methods.
- It is Difficult to produce parts with high thickness and diameter ratio. There are also limitations on particle sizes to produce homogeneous densities. Powder metallurgy can produce parts up to 20 kg.
- Lower mechanical properties may occur from time to time due to the existence of pores in the microstructure as compared to other approaches.

- The cost of the molds required for production is high.

## 3.3. CHARACTERIZATION OF POWDERS

### 3.3.1. Powder Sampling

Powder sampling, can be accomplished using a variety of methods. The commonly used method is to blend and apply small samples from many different points. The general form of the particles is cohesive, the tendency to stick to each other is high. Eventually agglomeration of particles is possible. High agglomeration may occur due to surface moisture. In addition, clinging agglomerates are characterized as a set of particles clinging to weak forces that can be destroyed by small shear stresses. For most particles, mechanical and ultrasonic agitation methods, surfactant liquids play an active role in dispersing the particles and subsequently determining the properties [65].

### 3.3.2. Particle Size Measurement

Particle size calculation and detailed information are necessary for researchers working on powder. Determining the particle size is not a simple task unless the particle is in spherical shape. In order to calculate particle size, it is mostly based on the geometrical structure of the particle and the diameter feature can be used. The size of the powder particles is determined by sieving or other methods. Not all powder particles have the same size. The particle size is determined using the average particle size property. If the particle geometry of the powder is complex, particle size measurement techniques also vary [66].

If powder particles are found mixed with powders of different sizes, four to five dimensional measurements are required. If its complex structure is dense, the particle size can be determined based on the surface area. The grain sizes of the powder particles are generally determined by the sieve analysis measurement method. The size of the sieve is calculated by the large hole in its structure. The calculation process is determined by the mesh method. According to SI, the size of the sieves is measured in

microns. The sieve method does not measure the actual size of the powder particle, it only classify it as greater as or smaller than a certain value [67].

### 3.3.3. Powder Mixing

Since powder mixtures are generally used in the powder metallurgy method, it is important to mix the powders effectively before they are subjected to the compaction technique. The homogeneity of the powder particles is the main purpose of the mixing process. Homogeneous mixing of powder particles of different sizes, forms and densities increases the performance of the result product.

When there are no standard dispersions in the powder mixture, blending should be performed before the mixing process. Blending is recommended in order to improve pressing and sintering properties and to produce a uniform size distribution. There are some factors affect the mixing and blending process. These factors are:

- Physical characteristics of powders.
- Mixer dimensions.
- Mixing speed.
- Mixing time.
- Powder volume in the mixer.
- Humidity and atmospheric conditions.
- Rotation speed.

There are various methods for the preparation of powders. These methods are divided into two main axes as mechanical and physio-chemical. Techniques used in the production of metal powders reveal many properties of powder particles. The powder particles produced with the requested specifications can be weighed by means of precision scales and the pressing process can be started directly, or the requested amounts of powder are included in the process in the mixing mills and made suitable for the pressing process. Production techniques are performed depending on the quality of metal powders. Economy is one of the most important factors in production technique.

### 3.3.4. Powder Compaction (Pressing)

When the metal powders are formed by means of a mold, it is desired that the powder fills the mold very well. When the powders are cold pressed in the mold, it is considered to reach the theoretical density as much as possible. Although the same pressing pressure is applied, the density reached after pressing in each metal powder is different according to the theoretical density of the material. The factors that depend on this condition are the shape of the powder, the grain size and surface, the type of material (production methods, specific surface) and the pretreatment applied to the powder [7].

Pressing is generally done by specially prepared steel molds at room temperature values. In mold manufacture process, cemented carbide-based and heat-hardened tool steel is used. The amount of pores differs depending on the pressing pressure, and the amount of pores decreases as the pressure ratio increases. However, depending on the rising pressing pressure, the amount of powder in contact with each other and the surface area increase. As the amount of pores increases, its density decreases. The tensile strength of the parts produced by powder metallurgy method varies depending on the amount of pores. As the density ratio increases, the tensile strength ratio also increases [68].

Compressing powders looks simple when observed from the outside. But on the contrary, it is a complex process with many parameters. The amount of friction that occurs on the inner surface of the mold when compression begins is greater than any other force that occurs. However, it appears to decrease slowly as it moves towards the center of the mold. Due to the friction between the mold surface and the powder, significant losses in forming energy occur. In addition, frictions arise between the contacting particles, between the balls and the mold surface, and between the powder and the balls. The friction that will occur between the inner surface of the mold and the product while being removed from the mold is extremely important. For these reasons, what is needed is a lubrication system that will not disrupt the sintering process in order to be effective in the forming and demoulding process [7].

The density of the powders placed into the mold before pressing is increased by the vibration of the mold. Increased density gained with vibration is related to the distribution scheme of the powder and the shape of the powder. This increase is much higher in powders with irregular shape compared to powders with smooth and spherical surfaces. The reason of this can be explained by the high density ratios based on spherical shaped powders and the low relative densities of irregular shaped powders with narrow powder size distribution. The ratio of the raw density to the theoretical density is expressed as relative density [7].

When discussing the pressing process generally, there are two types of pressing: cold pressing and hot pressing. In hot pressing processes, heat and pressure are applied at the same time, while in cold pressing processes, heat is applied after pressing. Cold or hot isostatic pressing methods are considerably superior to the pressing method by rigid molds in terms of providing good mechanical properties and measurement accuracy in the product. In the mentioned pressing methods, high wet density and high wet strength values can be obtained even at low pressure, since the pressure applied on the powder masses is distributed at the same rate. The materials produced by the hot isostatic pressing method, have pretty good mechanical properties such as tensile strength and fatigue strength. Cold and hot isostatic pressing are explained in the following headings [69].

#### 3.3.4.1. Single-action Die Compaction

Conventional powder compression processes are performed uni-axially. Immediately after the powder mixture is added into the mold, pressing processes are applied by the upper pressure plate such as shown in Figure 3.5. The purpose of using the lower piston is to scrape the resulting part from the mold. In order to facilitate the removal of the part from the mold and to provide the compression, lubrication is applied to the mold walls. As the amount of pressure applied in the single action compaction process is increased, the density of the compressed material also increases. The reason of this is the decrease in the pores among the powders used, as well as the fact that the mass remains the same but the volume decreases. Despite the advantages of this method, it

is not preferred because it cannot reach the expected density in intricately shaped parts and metallic parts with a high length/width ratio.

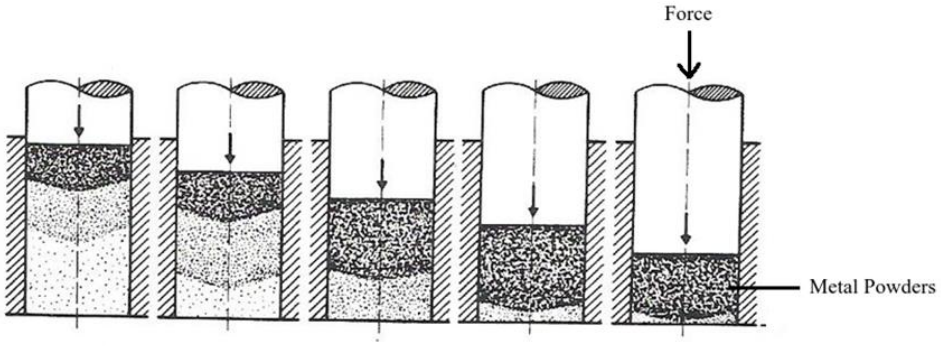


Figure 3.5. Single action die compaction [70].

### 3.3.4.2. Double-action Die Compaction

Pressure is applied by upper and lower punches to the die as shown in Figure 3.6. Both punches are dynamic. Punches can apply different or equal amounts of movement and pressure. The raw density distribution can vary significantly due to friction between particles, punches, powder particles and the mold surface. Some attempts are made to reduce these properties by reducing friction by using a lubricant or by using suitable compression methods.

It is not possible to reach full density through the single action compaction method. In double action compaction, since the powder is compressed by the upper and lower punches, the friction force between the wall of the mold and the powder particles exceeds the spring force of the flexible material such as the spring on the mold base, allowing the mold to move towards the lower region, allowing the lower punch to press the powder on the base surface of the powder with the upper punch with equal intensity. After the compression process is completed, the resulting part is stripped from the mold by the movement of the lower punch towards the upper section. As a result, it turns out that the density distribution is more homogeneous than the parts obtained by the single action compaction. The lowest density value is found at the midpoint of the compressed part. The distribution of this density is symmetrical [71].

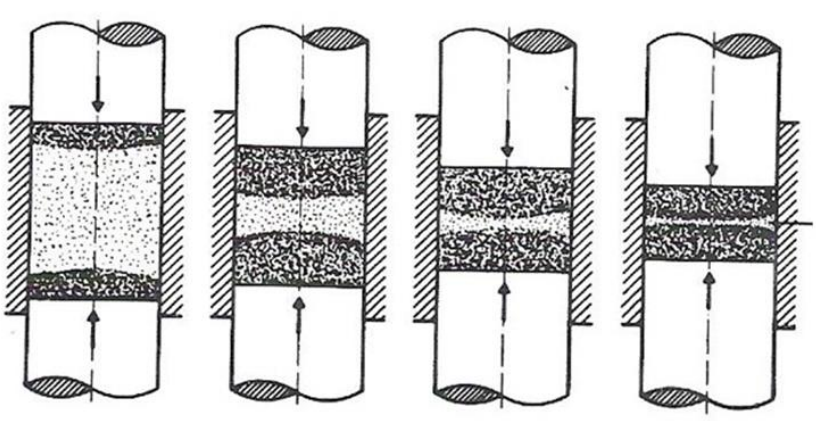

Figure 3.6. Double action die compaction [70].

### 3.3.4.3. Cold Isostatic Pressing

In this method pressures are applied equally from all directions. Cold isostatic compression (Figure 3.7) can be applied to complex and stepped parts with large aspect-to-diameter ratios. The powder is placed in a closed sealed elastic container that acts as a mold. The air in the soft mold is evacuated beforehand as it will come out during compression. The mold is immersed inside the pressure vessel by pumping liquid into the vessel. High pressure is applied to the fluid and the mold is left under hydrostatic pressure. After the pressing process is completed, the flexible mold is removed from the part and is usually not reused again after that. A more homogeneous density distribution can be obtained in the powder metal parts produced in this method [72].

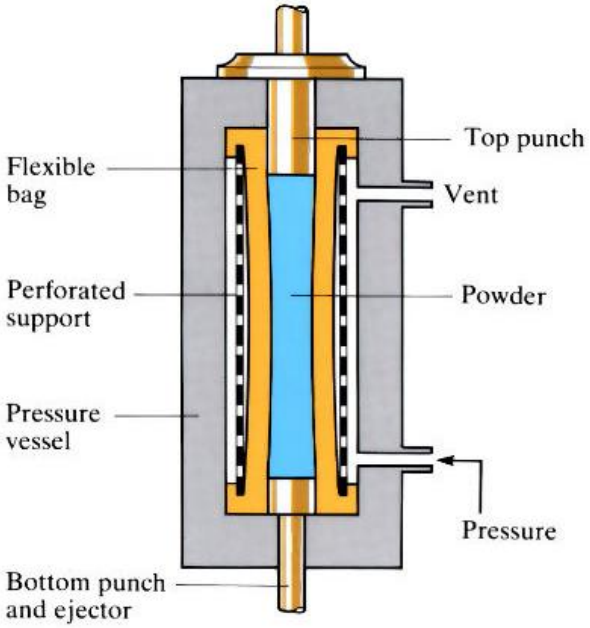


Figure 3.7. Cold isostatic pressing [73].

### 3.3.4.4. Hot Isostatic Pressing

The material blocks required to produce powder metallurgy parts with hot isostatic compression method are obtained by atomizing powder metals with inert gas. Metals that are very difficult to produce with conventional production methods, have very special properties, and cannot otherwise be mixed with each other, can be only produced by combining metals in powder form or using different powdered metal layers. Metal powders are filled into capsules, which are then loaded into a hot isostatic compression furnace (autoclave). Here the capsules are exposed to the high pressure and high temperature provided by the compressed inert gas. Although the pressure and temperature depend on the type of material, it is around 2000 bar pressure and 1400°C. The powders in the sealed capsule combine under isostatic gas pressure and high temperature and have a completely dense structure (Figure 3.8). Since the spaces between the powder particles are completely removed, the resulting compressed part has a completely non-porous structure. Hot isostatically compressed powder metallurgy produced parts are an extremely economical method for applications involving high temperatures, high mechanical stress, high corrosions stress and high wear [72].

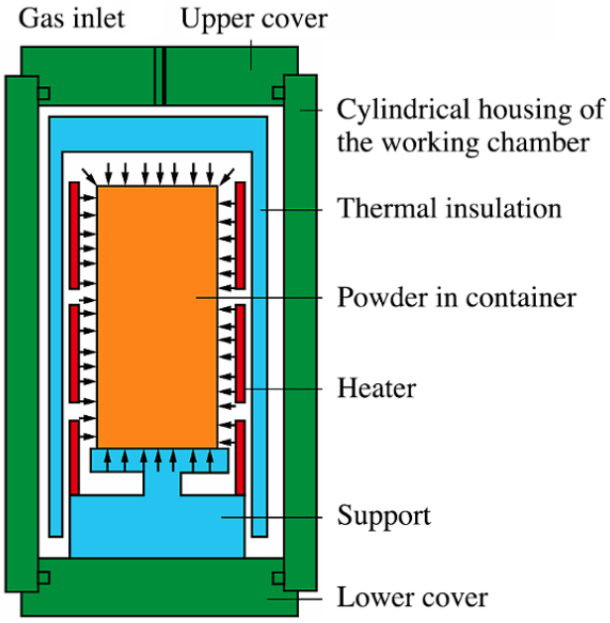


Figure 3.8. Hot isostatic pressing [74].

## 3.4. MACHINING

### 3.4.1. Chip Removal Mechanics and Chip Formation

Since the machining process is actually three-dimensional and quite complex, the two-dimensional orthogonal model given in Figure 3.9 is used to describe the machining mechanics. This model has a critical role in the analysis of the machining process and describes the mechanics of machining accurately and comprehensively. Orthogonal cutting model uses a wedge-shaped tool in which the cutting edge is orthogonal to the cutting direction. As the tool is forced into the workpiece, the shear deformation along shear plane oriented at an angle with the surface of the material creates the chip, this angle is called (shear angle). Plastic deformation occurs along the shear plane [75].

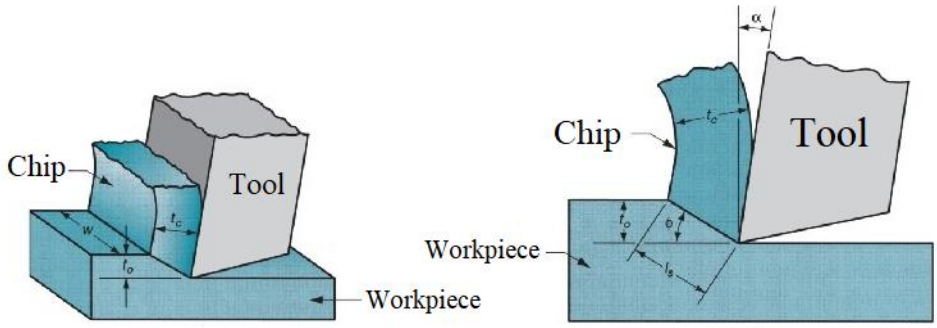


Figure 3.9. Orthogonal cut model [76].

Plastic deformation plays a critical role during chip formation in the manufacturing process. The region that occurs in a very narrow region with the regional deformation of the workpiece in front of the cutting tool and occurs in the shear plane is called the first deformation zone. The primary zone of deformation is the plastic deformation zone ahead of the cutting tool edge, and the secondary zone of deformation is the deformation zone on the back surface. The stress formed in the workpiece as a result of the relative movement between the tip of cutting tool and the workpiece causes the chip formation by plastically deforming the workpiece in the primary deformation zone. The layer removed from the workpiece undergoes a second deformation by slipping and sticking as the tool passes over the back surface, this region is called the secondary deformation zone. The region formed by the effect of friction caused by the contact of the chipped surface and the lateral surface of the cutting tool is defined as the tertiary (third) deformation zone. The third deformation zone is defined as the zone where the surface quality of the workpiece is affected. Chip formation process is shown in Figure 3.10 [75].

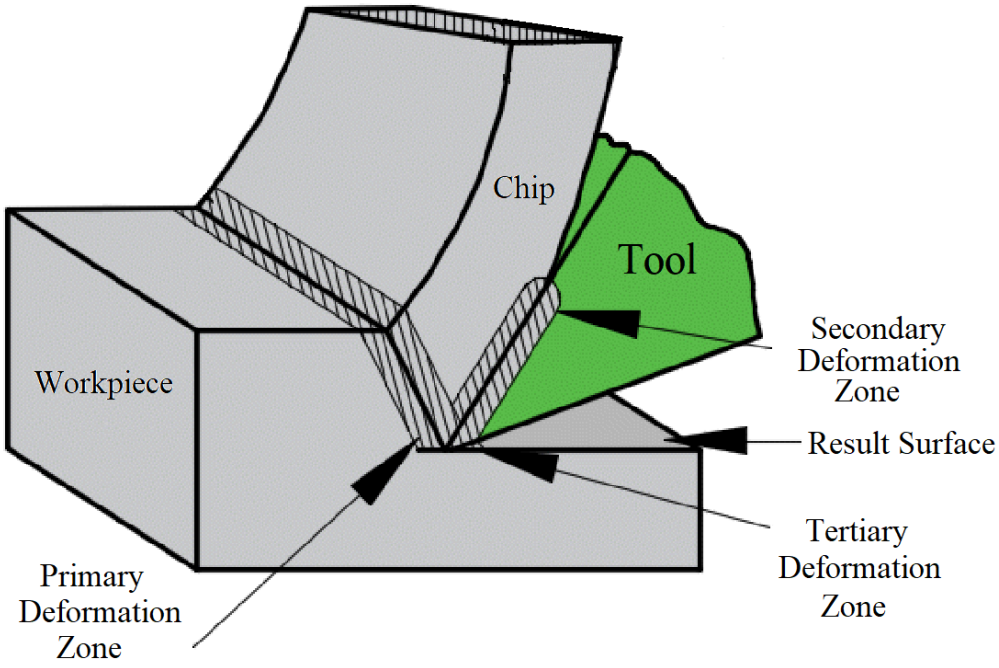


Figure 3.10. Chip formation [75].

### 3.4.2. Shear and Cuttıng Forces

It is known that the cutting forces generated during chip removal have a significant effect on the cutting performance, the quality of the machined surface and the unit cost of the part. Cutting forces are also considered in the design of cutting machine parts, in order to produce vibration-free and rigid cutting machines. In addition, it is used to determine the energy consumed by the cutting machine during chip removal from the workpiece. The cutting forces occurs in the turning process are shown in Figure 3.11. These forces applied on the cutting tool constitute an important stage of chip formation. The main cutting force ($F_c$) acts in the direction of the cutting speed and is important to determine the power requirement in metal cutting. Feed force ($F_f$), is the force acting in the direction of the cutting tool and is approximately 50% of the cutting force. The final component is radial (passive) force ($F_r$) it act perpendicular to the machined surface, it is approximately 50% of the feed force [75].

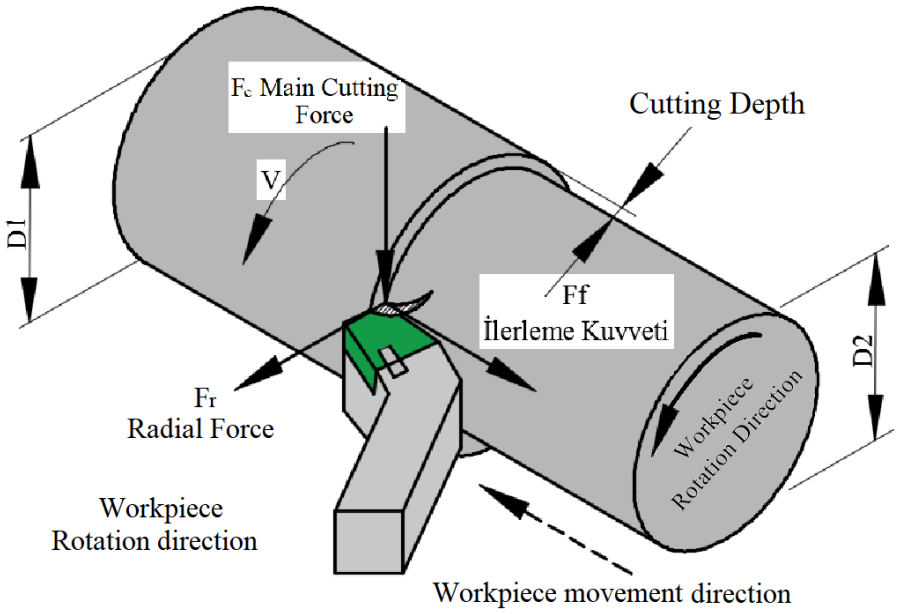


Figure 3.11. Cutting forces in machining process [75].

In order to achieve, high quality, safe and economical machining solution, all the acting forces must be measured properly. For this reason, measurements taken from the dynamometer are used to determine the cutting forces, and also mathematical models are developed based on these measurements [75].

### 3.4.3. Heat and Temperature

Almost all of the power used in cutting metals is converted to heat near the tool tip. Therefore, heat generation and temperature in the cutting zone are important factors in chip removal. The analysis of the heat generated in terms of cutting tool performance and workpiece quality is important [75].

The heat generated in metal cutting has a significant effect on tool life. Most of the heat generated is ideally reduced in the cutting zone by chipping. The amount of heat reduced varies depending on factors such as workpiece material, machining parameters, cutting tool material and geometry. Leakage of high amounts of heat to the workpiece or cutting tool in reduces the efficiency of the cutting process [75].

It is known that the cutting speed significantly affects the heat generated during the cutting process. With the increase of the cutting speed, the energy per unit time increases and this increases the heat and therefore the temperature. High temperature is one of the main factors limiting tool life and cutting speed. In this context, cutting tools manufacturers have focused on improving the ability of cutting tools to maintain their properties at high temperatures [75].

### 3.4.4. Surface Quality

Dimensional accuracy and surface quality are important considerations in the part manufacturing using machining methods. At this point, it is stated how the surface treatment marks, size and shape tolerances and the processing quality of the part will be determined. In particular, surface quality is important in applications where corrosion resistance, fatigue strength and wear life are sought. Moreover, surface quality affects various functional properties of parts, such as wear, light reflection, heat conduction, coating or resistance life, which causes friction of a part under operating conditions. Therefore, it is important to determine the ideal levels of parameters such as depth of cut, cutting speed, feed rate and cutting tool geometry, which have a direct effect on the surface roughness during machining in order to obtain the desired quality during the manufacturing phase of a part [75].

# PART 4

# MATERIALS AND METHODS

## 4.1. PRODUCTION PROCEDURE OF PM STEELS

In this study, PM steel samples containing molybdenum and chromium were produced in desired compositions by powder metallurgy (PM) method. The purities and sizes of graphite+ Mo, Fe, and Cr powders are given in Table 4.1. Powders are weighed using RADWAG AS-60-220 C/2 scale which is shown in Figure 4.1 with 0.0001 precision.

Table 4.1. Sizes and purity of the powders used in the study.

| Id. No | Elemental Powders | Powder Size (µm) | Purity (%) |
|---|---|---|---|
| **1** | Fe | <150 | 99.9 |
| **2** | C | 10-20 | 96.5 |
| **3** | Cr | <45 | 99.8 |
| **4** | Mo | <150 | 99.9 |
| **5** | 316L | <150 | 99.9 |

Figure 4.1. RADWAG AS-60-220 C/2 scale.

After the powder weighing process, the powder compositions in Table 4.2 were placed in a turbula mixer for two hours without adding metal balls. The turbula mixer is shown in Figure 4.2. In the next step, the mixed powders and 316L powder have been cold pressed unidirectionally under 700 MPa and then Sintered at 1400°C. The sintering process is carried out in an atmosphere-controlled tube furnace which is shown in Figure 4.3. The sintering process have been done with a gas circulation contain mixture of 95% nitrogen and 5% hydrogen, and a heating speed of 5°C per minute. After waiting for 1 hour, the furnace temperature is reduced at a speed of 5°C per minute. The sintered specimen is shown in Figure 4.4.

Table 4.2. Chemical compositions of the Cr-Mo steel produced using PM method.

| Alloys | Graphite (%wt.) | Cr (%wt.) | Mo (%wt.) | Fe (%wt.) |
|---|---|---|---|---|
| **0.55Graphite-Fe** | 0.55 | - | - | Rest |
| **0.55Graphite-Fe-1Cr** | 0.55 | 1 | - | Rest |
| **0.55Graphite-Fe-1Cr-0.5Mo** | 0.55 | 1 | 0.5 | Rest |
| **0.55Graphite-Fe-3Cr-0.5Mo** | 0.55 | 3 | 0.5 | Rest |
| **0.55Graphite-Fe-1Cr-5Mo** | 0.55 | 1 | 5 | Rest |
| **0.55Graphite-Fe-3Cr-5Mo** | 0.55 | 3 | 5 | Rest |
| **0.55Graphite-Fe-1Cr-10Mo** | 0.55 | 1 | 10 | Rest |
| **0.55Graphite-Fe-3Cr-10Mo** | 0.55 | 3 | 10 | Rest |

Figure 4.2. Turbula triaxial mixer.

Figure 4.3. Atmosphere-controlled tube furnace.

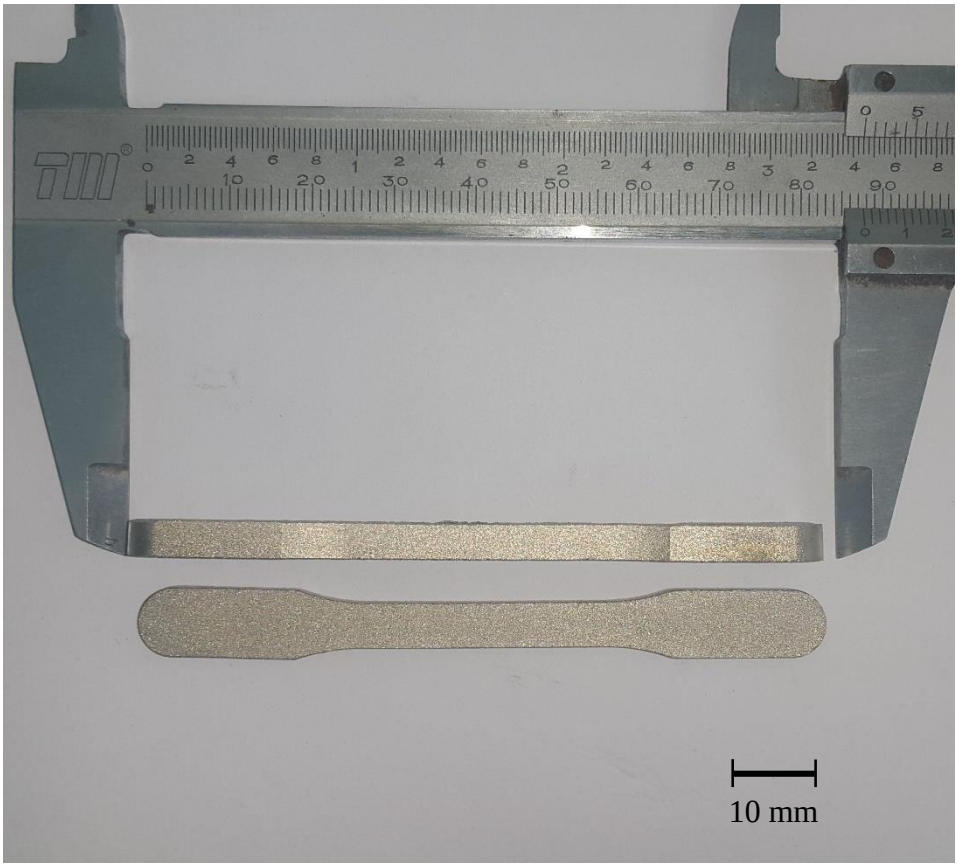


Figure 4.4. Schematic view of produced samples.

Tensile tests were applied to samples at a tensile speed of 1 mm/min using a SHIMADZU tensile tester machine shown in Figure 4.5. Consequently, the tensile strength, yield strength and elongation values of produced steel samples were obtained. At the same time, hardness tests were conducted using a hardness measuring device. $HV_{0.5}$ (500g) load was used for the measurement process. Five measurements were made for each sample and the average of these measurements was adopted as the hardness value for this sample. After that microstructural examinations were performed with an optical microscope at X50-X1000 magnification.

The size and type of the precipitates were also determined by performing SEM/EDS analyses. The microstructural change has been used to explain the change in mechanical properties of the produced samples. Figure 4.6 shows the schematic view of the production and milling stages of Cr-Mo steels with the PM method.


Figure 4.5. SHIMADZU tensile test machine.

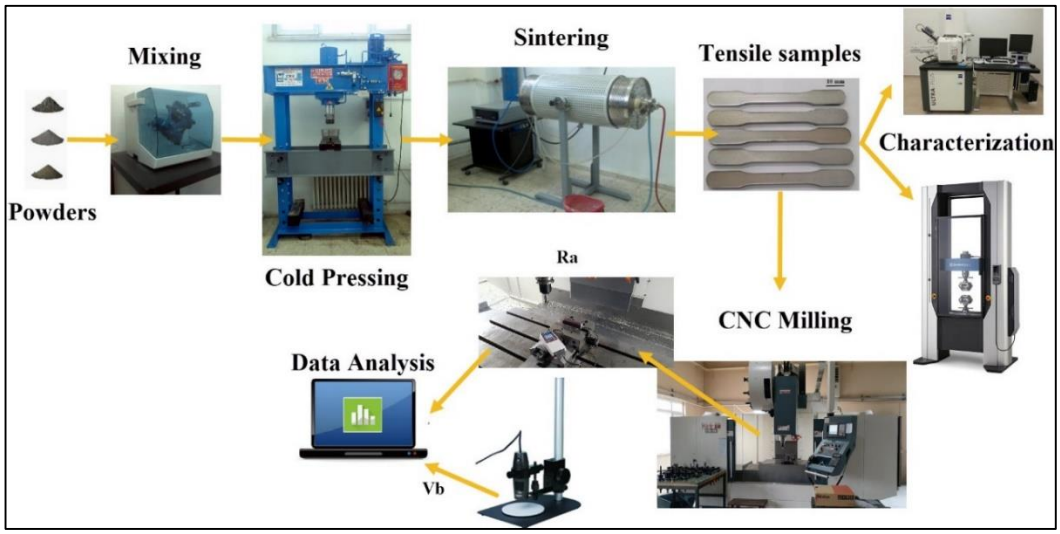


Figure 4.6. The production and milling stages of Cr-Mo steels with the PM method.

## 4.2. MILLING EXPERIMENTS

The milling tests were performed on Hannsa YH1600-A CNC milling machine at three different feed rates (0.4, 0.6, and 0.8 mm/tooth), three different depths of cut (0.5, 0.7, and 0.9 mm), and three different cutting speeds (120, 180, and 240 m/min).

Walter SDMT06T204-F57 WKP35S cutting inserts and M4132-025-W25-04-06 shoulder milling cutters were used in the milling tests. The inserts have a corner radius of 0.4 mm and are coated with CVD-TiAlN+TiCN coating.

## 4.3. SURFACE ROUGHNESS (RA) AND FLANK WEAR (VB) MEASUREMENT

Roughness measurements of the machined surface were performed after each experiment using a Mitutoyo surface roughness tester. The assessment length and cut-off length were chosen at 0.8 and 12 mm, respectively. The Ra values were obtained by taking the average of three values measured from three different points of the machined surface.

A scanning electron microscope (SEM) was used to inspect the worn cutting inserts. A digital microscope was also used to measure the flank wear (Vb) of the worn cutting

tools. The uniform flank wear value was determined as 0.3 mm according to ISO-8688 [77]. The cutting inserts were checked after each predetermined cut-off length (80 mm) and the cut length was specified as 400 mm.

## 4.4. CORROSION TEST

### 4.4.1. Samples Preparing

For the corrosion tests, the samples must be cut and shaped in a special way. The surfaces of the samples that will come into contact with the liquid in the corrosion tests are prepared and the surface area was measured. To connect our samples to the electrochemical corrosion tester, a copper wire cable was attached to the top surface of the samples. Cutting and shaping process was done using Metacut 251 brand cutting machine which is shown in Figure 4.7.


Figure 4.7. Metacut 251 cutting machine.

### 4.4.2. Corrosion Test

A potentiostat corrosion test device was used to perform the corrosion tests. Before explaining the used equipment, the general working principle of the potentiostat will be explained.

#### 4.4.2.1. Potentiostat and Three Electrode Cells Working Principle

Potentiostat is an electronic device that controls the voltage difference between the Working Electrode (1st electrode) and the Reference Electrode (2nd electrode). Both electrodes are housed in an electrochemical cell. Potentiostat can provide this control by giving current to the cell via an Auxiliary or Counter Electrode (Counter/Auxiliary) (3rd electrode). Potentiostat measures the current that will occur between the Working Electrode and the Counter Electrode (3rd electrode). By measuring this current, the chemical reactions and interactions that may occur on the Working Electrode will be measured. The variable to be controlled in a potentiostat is the cell potential. The variable to be measured is the cell current [42]. The scheme of the electrochemical cell is shown in Figure 4.8.

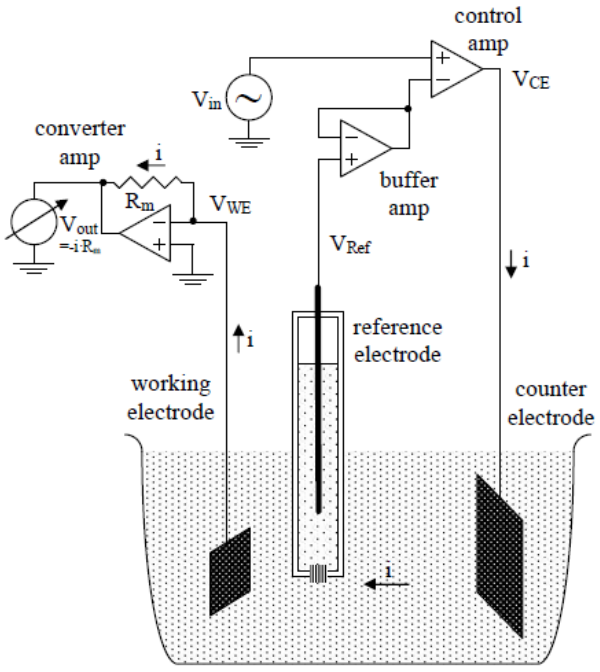


Figure 4.8. Electronic schematic of electrochemical cell [78].

In this work the PARSTAT 4000 brand potentiostat measurement system located in the Corrosion Laboratory of the Iron and Steel Institute was used. The device is shown in Figure 4.9.


Figure 4.9. PARSTAT 4000 Potentiostat [79].

This device was used to perform a potentiodynamic corrosion test using the parameters shown in Table 4.3 in room temperature (25 ºC).

Table 4.3. Potentiodynamic corrosion test parameters.

| | |
|---|---|
| **Corrosion test** | Potentiodynamic |
| **Open circuit potential (OCP) measuring time** | 300 s |
| **Scan rate** | 1.5 mV/s |
| **Reference electrode** | Ag/AgCl |
| **Counter electrode** | A pair of graphite rods |
| **Electrolyte (Corrosive environment )** | PBS |

#### 4.4.2.2. Body Fluid Simulation

In corrosion tests performed on medical implants, compounds called simulated body fluids (SBF) are used. In this work Phosphate Buffered Saline (PBS) with 7.4 pH was used to simulate body fluids inside the human body. The volume used in the experiments is 100 ml. the chemical formulation of PBS is given in Table 4.4.

Table 4.4. Chemical composition of PBS.

| Component | g/mol | Molar concentration (mM) |
|---|---|---|
| Sodium chloride (NaCl) | 58.44 | 137 |
| Potassium chloride (KCl) | 74.55 | 2.7 |
| Sodium phosphate dibasic dodecahydrate ($Na_2HPO_4$-$12H_2O$) | 358.2 | 10 |
| Monopotassium phosphate ($KH_2PO_4$) | 136.086 | 1.8 |

# PART 5

# RESULTS AND DISCUSSION

## 5.1. ASSESSMENT OF MICROSTRUCTURE AND MECHANICAL PROPERTIES

The tensile graphs obtained after the tensile test of the samples produced using the PM method are shown in Figure 5.1. In addition, elongation ratio, tensile strength, and yield strength values were obtained after this test for all samples are given in Table 5.1.

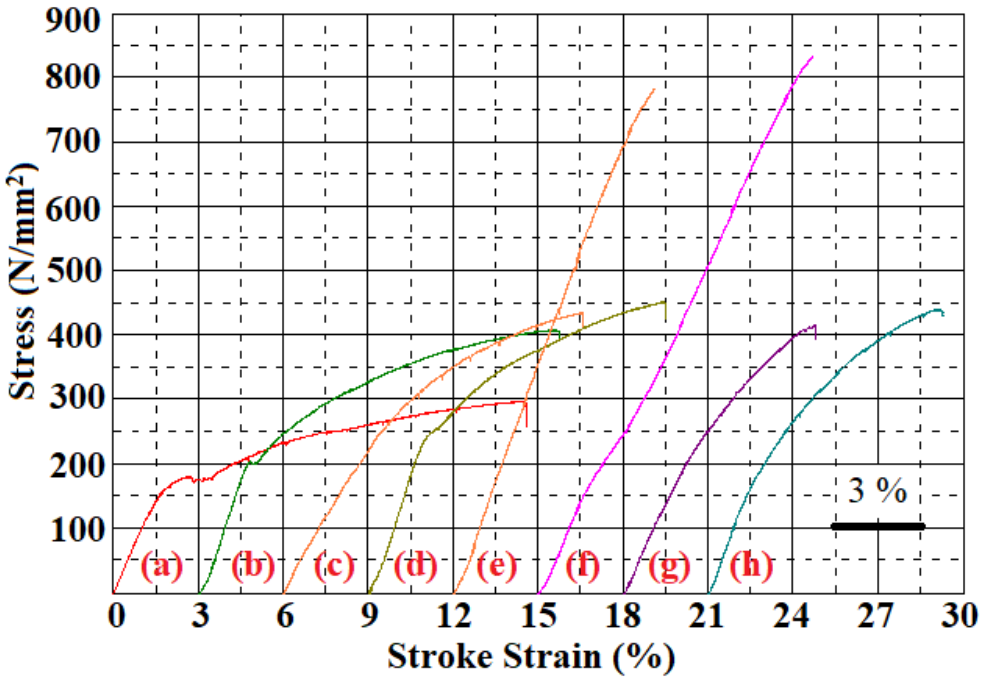


Figure 5.1. Difference of stress–strain curves of the unalloyed and alloyed PM Cr steels with different Mo a) Fe-Graphite, b) Fe- Graphite-1Cr, c) Fe-Graphite-1Cr-0,5 Mo, d) Fe- Graphite-3Cr-0,5 Mo, e) Fe- Graphite-1Cr-5 Mo, f) Fe- Graphite-3Cr-5 Mo, g) Fe- Graphite-1Cr-10 Mo and h) Fe-Graphite-3Cr-10 Mo.

Table 5.1. Mechanical properties of the Cr-Mo PM steels.

| Alloys | Yield strength (MPa) | Ultimate tensile strength (MPa) | Elongation (%) | Hardness ($Hv_{0.5}$) |
|---|---|---|---|---|
| **0.55Graphite-Fe** | 178 | 298 | 14.4 | 105 |
| **0.55Graphite-Fe-1Cr** | 208 | 410 | 12.6 | 119 |
| **0.55Graphite-Fe-1Cr-0.5Mo** | 221 | 436 | 10.6 | 133 |
| **0.55Graphite-Fe-3Cr-0.5Mo** | 254 | 455 | 10,4 | 150 |
| **0.55Graphite-Fe-1Cr-5Mo** | 411 | 783 | 7.1 | 227 |
| **0.55Graphite-Fe-3Cr-5Mo** | 488 | 836 | 9,7 | 255 |
| **0.55Graphite-Fe-1Cr-10Mo** | 219 | 417 | 6.8 | 125 |
| **0.55Graphite-Fe-3Cr-10Mo** | 233 | 442 | 8.1 | 135 |

As shown in Table 5.1 and Figure 5.1, when adding chromium at 1 and 3 percent of the total weight and molybdenum at 0.5 and 5 percent of the total weight to the Fe-Graphite main matrix composition, the tensile strengths increases, and the elongation ratio values decreases.

As seen in Figure 5.1 and Table 5.1, an overall increase in tensile strength and a significant decrease in elongation values occurs when 1% chromium and 0.5 and 5% molybdenum are added to the Fe-Graphite main matrix composition. This situation can be explained with strength-enhancing mechanisms such as precipitation hardening, aggregation hardening, dispersion hardening, and grain size reduction due to the formation of precipitates such as CrN, CrC, CrC(N), MoN, MoC, MoC(N) and CrMoC(N) formed at the matrix and grain boundaries during and after sintering. On the other hand, the addition of 10% by weight of Mo caused a tendency to decrease in the hardness, yield strength, and tensile strength of the samples. As seen in Figure 5.2 (g) and (h), it is thought that excessive accumulation of precipitates such as CrMoC(N), CrC(N), and MoC(N) at the grain boundaries may cause a decrease in strength. This situation was also reported by other researchers [80,81]. For example, Özdemirler et al. observed that the average grain size increases slightly with the

increase of NbC from 0.2% to 2% of the total weight. The excessive formation of large NbC precipitates at the grain boundaries, the inability of the carbonitrides formed to reduce the grain size sufficiently and the precipitate density formed at the grain boundaries making the grain boundaries more brittle is reported as the reason for this situation [81].

Figure 5.2 shows microstructure images of Cr-Mo steel samples. When Figure 5.2 is examined, it is observed that unalloyed PM steel is formed in ferrite and pearlite phases, and the grain size decreases with the addition of 1% Cr to the unalloyed steel sample, and the amount of pearlite increases. Moreover, the amount of perlite increased and bainitic phases were found in the microstructure with the addition of Mo to the steel samples containing 1% Cr [82,83]. When 10% molybdenum was added, a decrease in the bainite phase was observed as a result of the excessive formation of MoC(N) precipitates at the boundaries of the molybdenum grains in the microstructure, and as a result, there was a decrease in the hardness, tensile strength and yield strength. Furthermore, the samples containing 5% Mo with different Cr amounts are compared with each other, an improvement in the elongation values with the addition of chromium has been observed. With the addition of chromium, carbon accumulated in the free grain and at the grain boundaries and precipitate such as chromium and molybdenum elements CrC(N) and CrMoC(N) were formed and grain size thinning was observed. As a result, an increase in tensile strength, yield strength and elongation values was observed. Moreover, similar results are seen when steels containing 10% Mo are compared with each other.

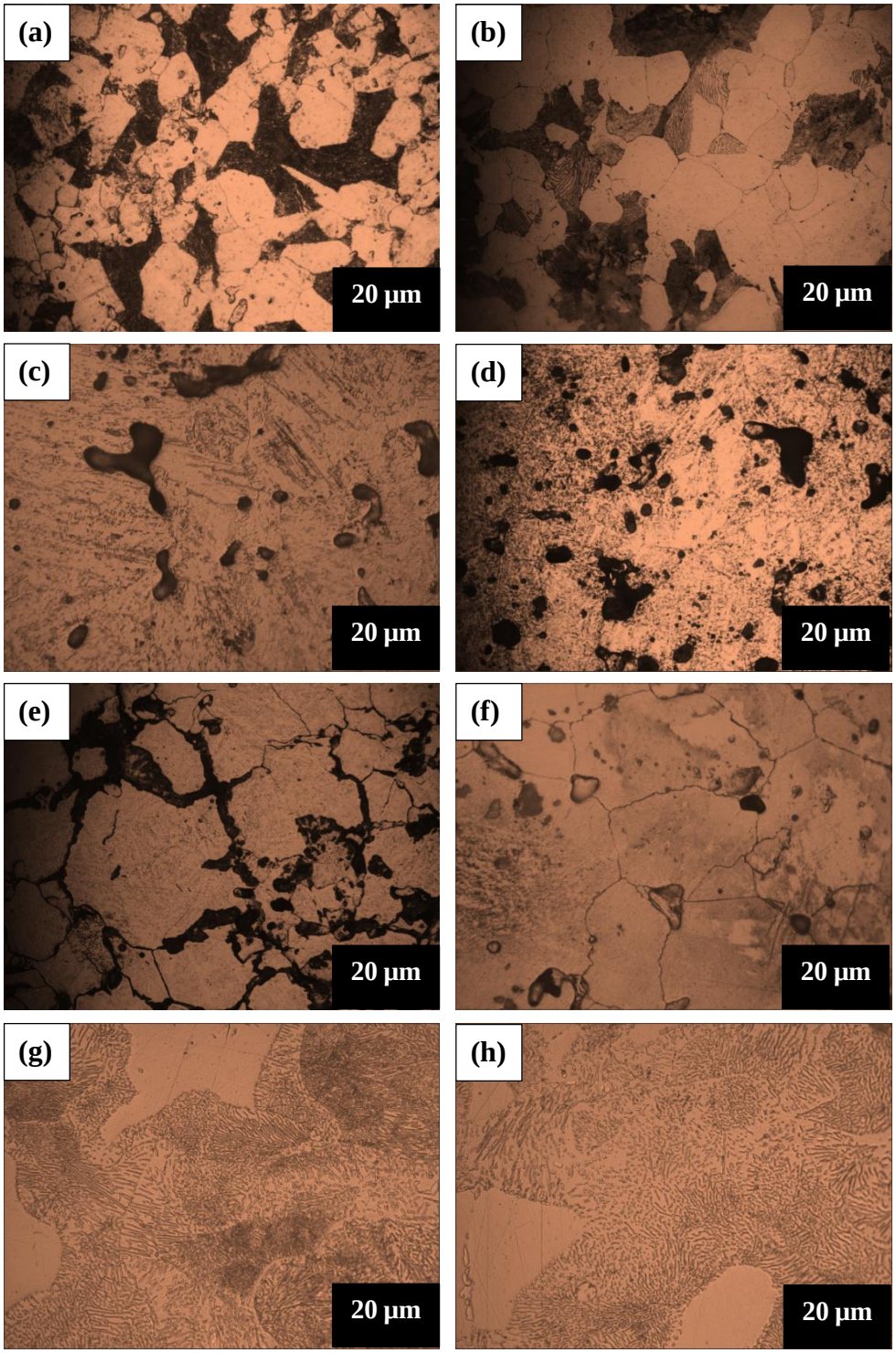


Figure 5.2. Microstructure images of PM Cr steels with different molybdenum ratios (500X) a) Fe-Graphite, b) Fe- Graphite-1Cr, c) Fe- Graphite-1Cr-0,5 Mo, d) Fe- Graphite-3Cr-0,5 Mo, e) Fe- Graphite-1Cr-5 Mo, f) Fe- Graphite-3Cr-5 Mo, g) Fe- Graphite-1Cr-10 Mo and h) Fe- Graphite-3Cr-10 Mo.

The results of SEM microstructure analysis and EDS analysis of steel samples produced by the PM method are shown in Figure 5.3. The presence of C, Fe, Mo, and Cr in the steel and the formation of nitride, carbide, or carbonitride precipitates such as CrC(N), MoC(N), CrMoC(N) and Fe3C were determined as a result of SEM microstructure and EDS analysis. These precipitates have been shown to limit the growth of austenite grains while also increasing the strength of the material through precipitation hardening [20].

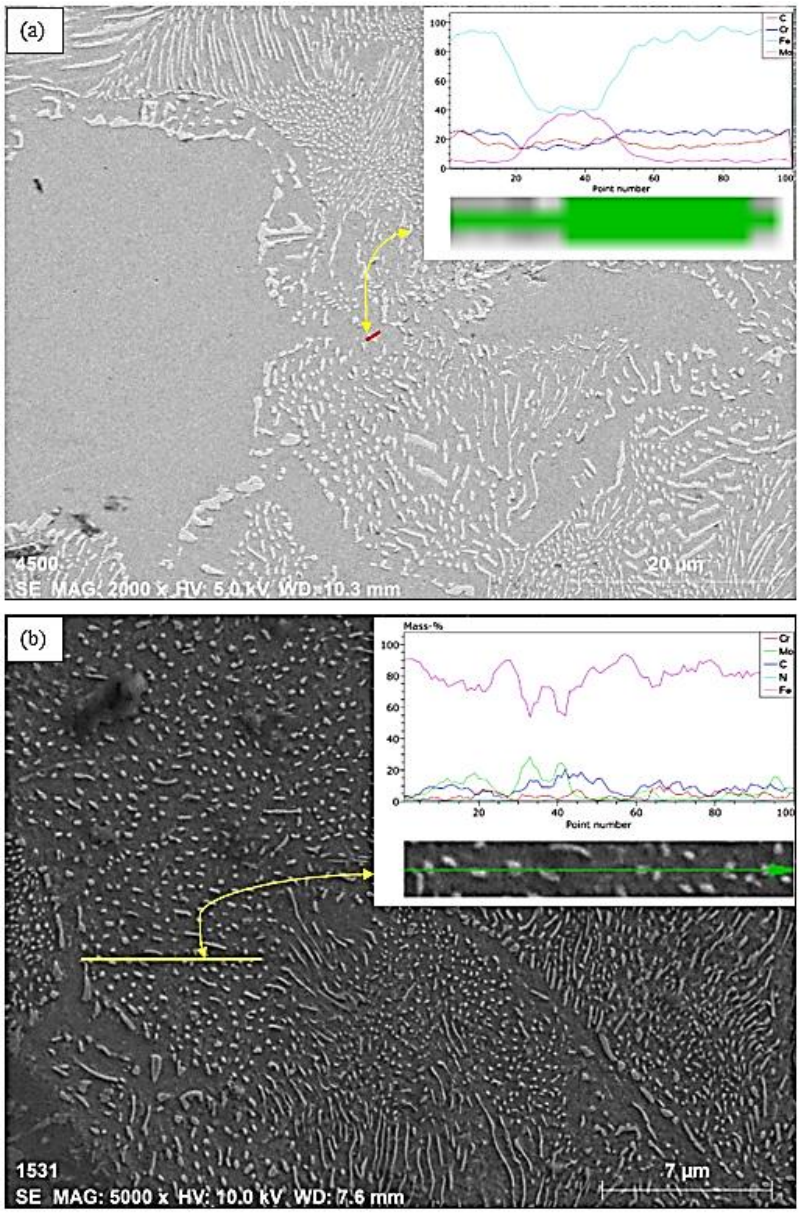


Figure 5.3. Microstructure images (a-2000X-b-5000X) and line EDS results of PM 3% Cr steel with 10% molybdenum.

The effect of alloying elements in solution on austenite recrystallization is relatively weak. The effect of precipitated particles on grain boundary movement is much more than that of dissolved atoms [84–86]. In the results of EDS analysis and microstructure SEM, it was determined that Cr and Mo elements were in composite and in the form of precipitated particles.

With the addition of Mo to Cr steel, precipitates such as CrC(N), MoC(N), and CrMoC(N) are thought to form in the microstructure, as shown in Figure 5.3. For example, SEM and EDSs taken from the microstructure support this. As shown by the EDS line taken from steel containing 10% Mo and 3% Cr of the total weight, the matrix phase was found to be rich in Fe, but the round-shaped precipitate was rich in molybdenum and chromium. In addition, a sharp increase in the amount of molybdenum and chromium was noticed when the analysis line from the matrix cut through the precipitate. When the analysis line cross the precipitate, there is an increase in iron and a decrease in chromium and molybdenum. When the line EDS result is evaluated, this precipitate is considered to be MoCrC(N) precipitate. When the line EDS analysis results obtained in this study are compared with the previous literature studies, it shows that precipitates such as MoC(N), CrC(N), and MoCrC(N) occur in alloyed PM steels. For example, Gündüz et. al. mentioned that the addition of % Ti-V increased the ultimate tensile strength and yield strength of PM steels due to the formation of TiC(N) and VC(N) precipitates [87]. On the other hand, Kostryzhev et al. mentioned that the effect of alloying elements in solution on austenite recrystallization is very weak. The effect of precipitated particles on grain boundary movement is much more than that of dissolved atoms [86].

Figure 5.4 shows the fractured surface images of the samples. When Figure 5.4 is examined, it was observed that the fractured surfaces exhibited partially brittle (separation planes) and partially ductile (honeycomb structure) behavior. Moreover, it was clearly seen that all the cracked surfaces had pores. This indicates that the fracture occurs by the merging and propagation of micro gaps. However, the separation planes, which are an indicator of brittle fracture, are seen to be highest in Cr steels containing 10% Mo of weight, moderate in Cr steels containing 0.5-5% Mo, and least in Cr steel without Mo and unalloyed steel samples. The samples also had large gaps in them. The

appearance of these gaps indicates that during the tensile test, precipitates such as MoC(N), MoCrC(N), and CrC(N) were separated from the surface [88]. Chandramouli and Shanmugasundaram associated this with the separation of nitride, carbonitride, and carbide from the surface during the tensile test [89]. To summarize, an increase in tensile strength and yield strength and a decrease in elongation values are observed with increasing Cr and Mo content and the values obtained as a result of tensile test are consistent with the fracture surface images.

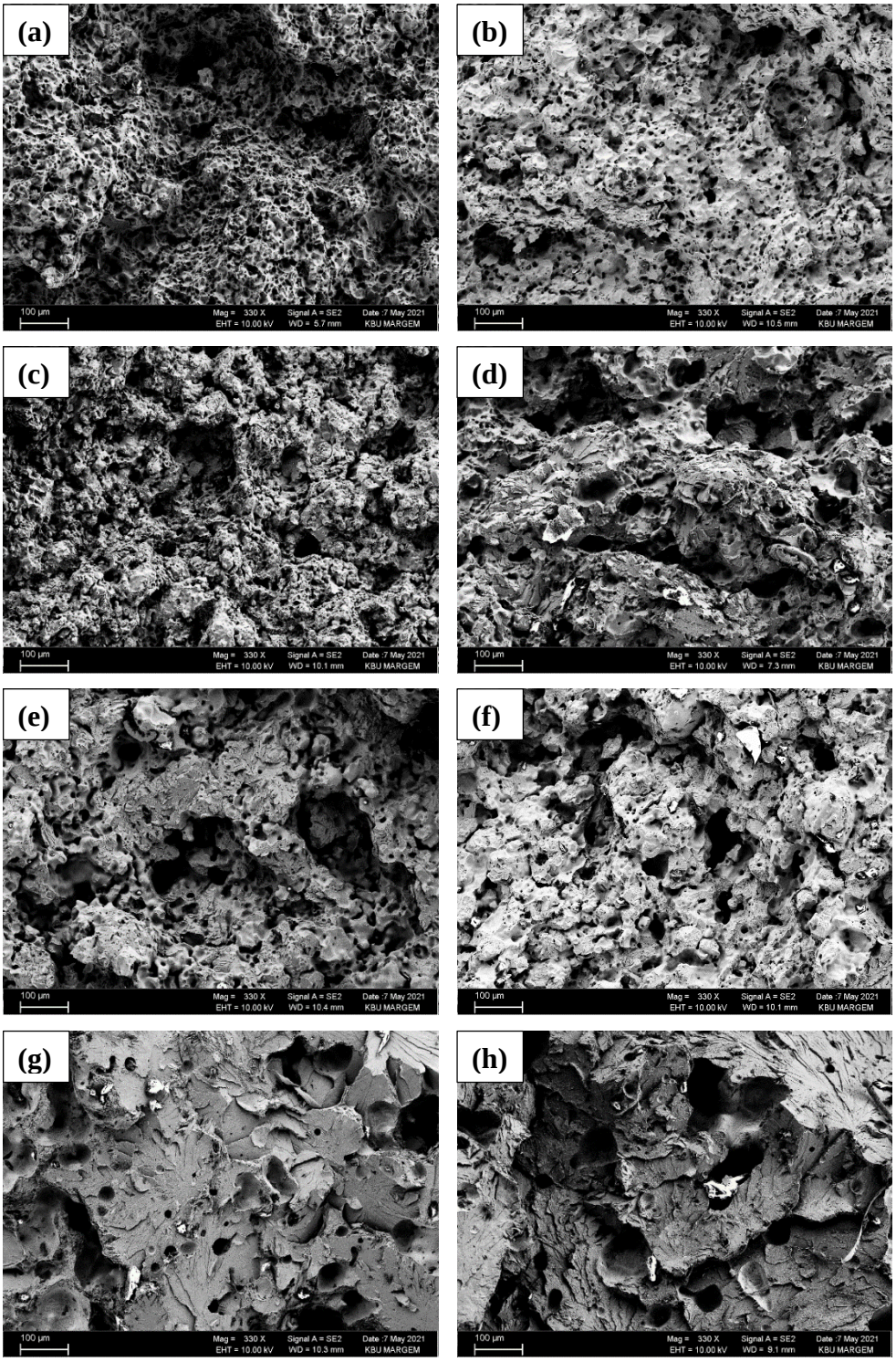


Figure 5.4. Fractured surface image of samples sintered at 1400 ºC at 330X (a) Fe-Graphite, b) Fe- Graphite-1Cr, c) Fe- Graphite-1Cr-0,5 Mo, d) Fe-Graphite-3Cr-0,5 Mo, e) Fe- Graphite-1Cr-5 Mo, f) Fe- Graphite-3Cr-5 Mo, g) Fe- Graphite-1Cr-10 Mo and h) Fe- Graphite-3Cr-10 Mo).

## 5.2. ASSESSMENT OF FLANK WEAR (VB)

The wear mechanisms were investigated using SEM to analyze the effects of Mo and Cr alloying elements on cutting tools. SEM examination revealed flank and nose wear as the dominant wear mechanism. The effect of Mo and Cr alloy elements on tool life was evaluated according to these two wear types. In this context, 0.5 mm depth of cut, 120 m/min cutting speed, and 0.4 mm/tooth feed rate were selected for the analysis of tool wear and the milling experiments were performed at constant cutting distance. The variation of flank and nose wear values are illustrated in Figure 5.5 for all alloys. In general, the lower flank and nose wear was achieved in the machining of Alloy I (0.55 Graphite-Fe). Furthermore, the Alloy II, Alloy III, Alloy IV, Alloy V, Alloy VI, Alloy VII, and Alloy VIII increased the flank wear by 20, 26.66 40, 96.6, 100, 33.33, and 40%, respectively in comparison to Alloy I. From this result, it can be deduced that Mo and Cr alloying elements increase tool wear. Moreover, it is seen that Alloy V and VI reach the wear criterion (0.3 mm) at a shorter cutting distance compared to other alloys. The fact that these alloys' tensile, yield strength and hardness are quite high compared to other alloys may be the reason for the increase in tool wear. The presence of precipitates such as CrMoC(N) and CrC(N) in these alloys is also thought to make machinability difficult. On the other hand, with 10% Mo addition in Alloys VII and VIII, the spread of precipitates such as MoC(N), CrC(N), and CrMoC(N) at the grain boundaries and accordingly a decrease in yield and tensile strengths had a positive effect on the tool life.

The SEM pictures in Figure 5.6 show the worn inserts at the end of all alloys cutting. When Figure 5.6 is examined, the addition of Mo and Cr in the samples strongly damaged the cutting edge and nose of the inserts. Furthermore, the grooves on the flank face and nose of the worn inserts obtained in the machining of Mo and Cr alloys are bigger than the worn insert obtained in the machining of 0.55 Graphite-Fe alloy.

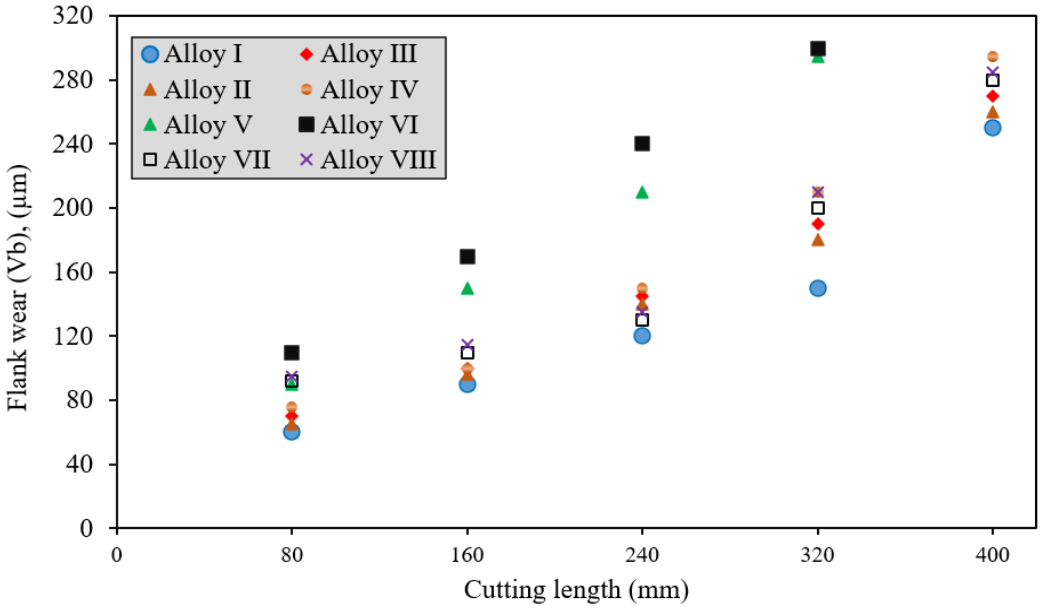


a)

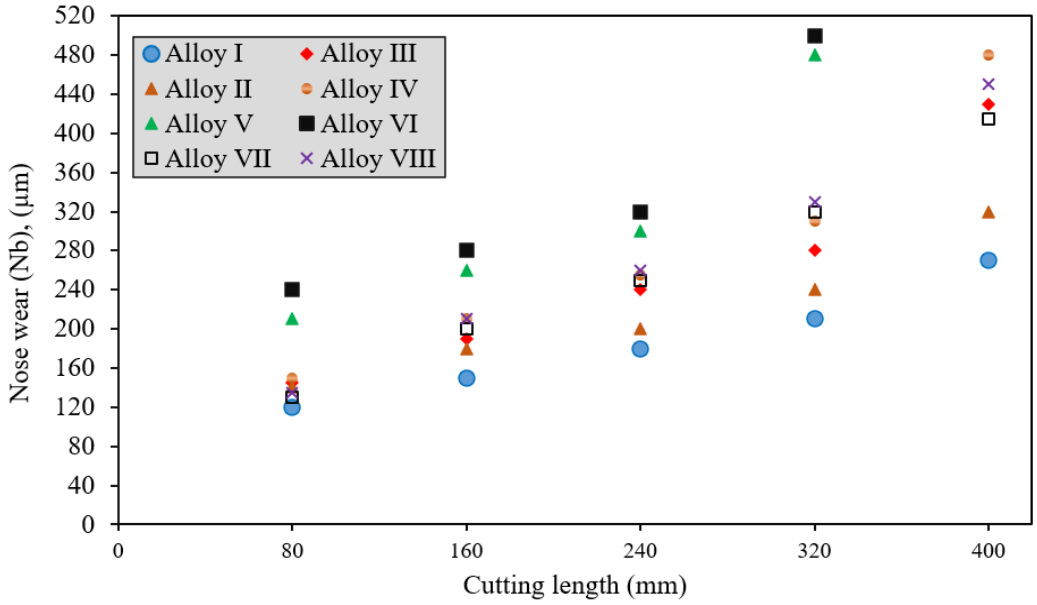


b)

Figure 5.5. Variation of tool wear results for all samples, a) Flank wear b) Nose wear.

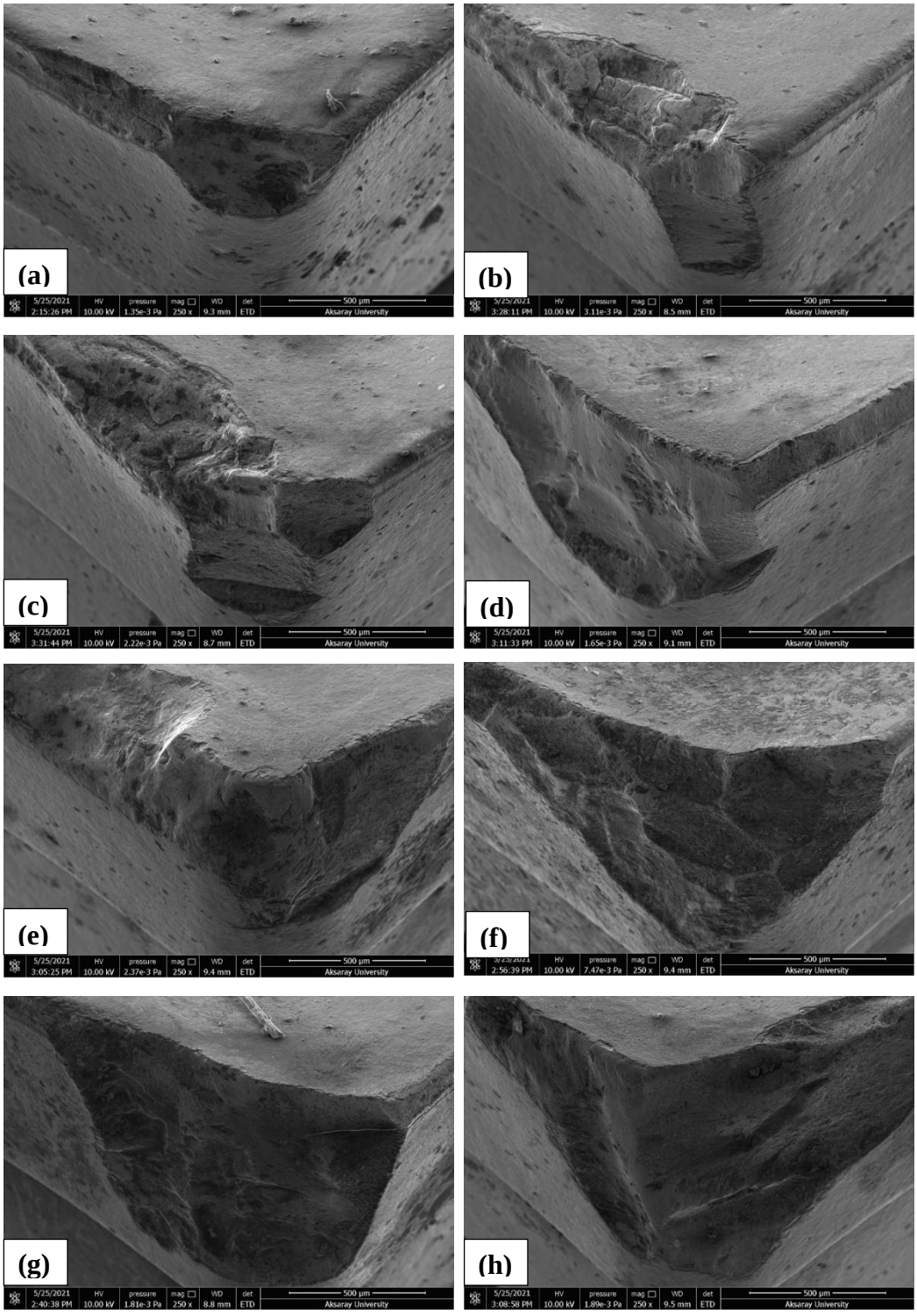


Figure 5.6. SEM images of the tool wear obtained from machining a) Alloy I, b) Alloy II, c) Alloy III, d) Alloy IV, e) Alloy V, f) Alloy VI, g) Alloy VII, and h) Alloy VIII.

## 5.3. ASSESSMENT OF SURFACE AVERAGE ROUGHNESS (RA)

The effects of alloying elements and cutting parameters on surface average roughness (Ra) have been investigated. Figure 5.7 illustrates the variation of the average surface roughness (Ra) values obtained when milling the samples. In general, the increase of the addition of Mo and Cr in samples resulted in the decrease of Ra. The lowest Ra values were measured in milling of Alloy VII and Alloy VIII and the highest Ra values were obtained in milling of Alloy I. For all alloys, the Ra values measured in the experiments performed under optimum cutting conditions of 0.5 mm depth of cut, 120 m/min cutting speed, and 0.4 mm/tooth feed rate were compared. To elaborate, the Alloy II, Alloy III, Alloy IV, Alloy V, Alloy VI, Alloy VII, and Alloy VIII improved surface quality about 5.38, 9.61, 21.15, 68.46, 70, 70.76, and 76.34%, respectively in comparison to Alloy I. Moreover, the lowest Ra value was measured as 0.415 µm in the machining of Alloy VIII containing 10% Mo and 3% Cr at a depth of cut of 0.5 mm, cutting speed of 240 m/min and a feed rate of 0.4 mm/tooth. As can be deduced in Table 3, the notable reason for the improvements with the addition of Cr and Mo alloying elements could be the easy removal of chips in the milling process with the increase in tensile strength, yield strength and hardness, and decrease in elongation ratio.

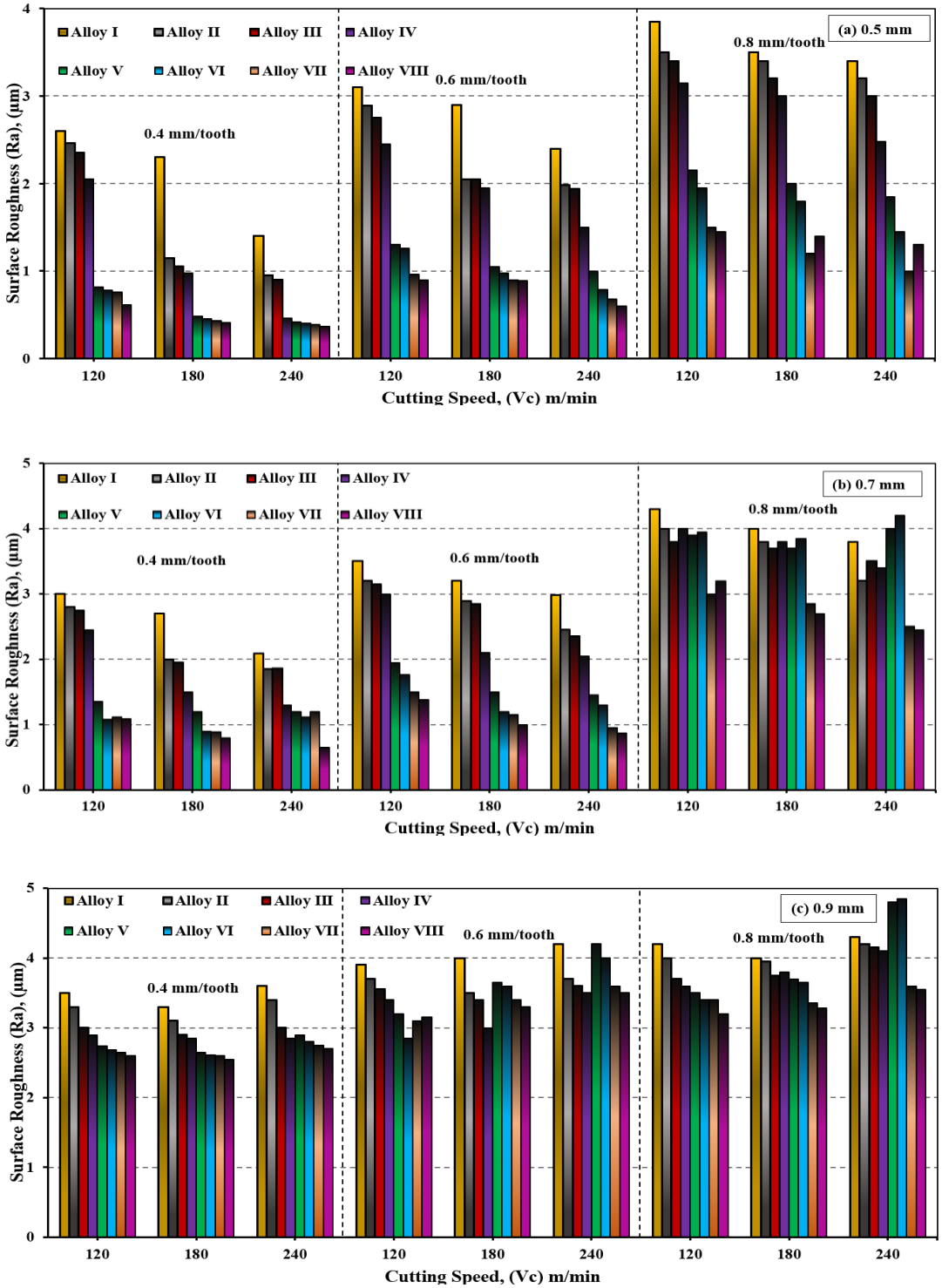


Figure 5.7. Variation of surface roughness results for all samples, a) 0.5mm b) 0.7mm c) 0.9 mm.

Considering the effect of the cutting parameters, on the other hand, it can be observed that the values of Ra decreased slightly with the increase of the cutting speed while it increased with the increase of the depth of cut and the feed rate. Moreover, the values of the surface roughness increased significantly in the experiments carried out at the 240 m/min Vc, 0.8 mm/tooth f, and 0.9 mm a (mm). For Alloy I, Alloy II, Alloy III, Alloy IV, Alloy V, Alloy VI, Alloy VII, and Alloy VIII, the surface roughness values were measured as 4.30, 4.20, 4.15, 4.10, 4.00, 3.98, 3.62, and 3.55 µm, respectively in the experiments performed on these parameters. The reason could be the tool enters the early wear process at the highest levels of cutting parameters. Furthermore, this supports the results obtained from worn cutting inserts images which showed high tool wear after machining at these parameters. The wear mechanisms in the cutting tool affect the surface roughness was also reported by other researchers [90,91]. In addition to the tool wear, the Ra is affected by several other factors such as cutting tool hardness, workpiece material hardness, cutting temperature, and friction [92].

## 5.4. OPTIMIZATION OF CUTTING PARAMETERS FOR RA AND VB

The optimization process aims to model the output parameters (Vb and Ra) and determine the most suitable input parameters. Therefore, the Taguchi L18 index was used in the design of milling experiments. Tensile strength values were considered in defining the workpiece material with a factor for the optimization process. In addition to workpiece material, factors B, C, and D are defined as, cutting speed, feed rate and depth of cut, respectively. The S/N ratios were calculated for each experimental combination, and the experiment results and the S/N ratios are given in Table 5.2.

Table 5.2. The experiment results and the S/N ratios.

| Test Id | Parameters | | | | | Vb-S/N (dB) | Ra (µm) | Ra-S/N (dB) |
|---|---|---|---|---|---|---|---|---|
| | A (Ct) | B (Vc) | C (f) | D (a) | Vb (mm) | | | |
| **1** | 298 | 120 | 0.4 | 0.5 | 0.28 | 11.0568 | 2.601 | -8.29947 |
| **2** | 298 | 180 | 0.6 | 0.7 | 0.30 | 10.4576 | 3.215 | -10.1030 |
| **3** | 298 | 240 | 0.8 | 0.9 | 0.34 | 9.3704 | 4.344 | -12.6694 |
| **4** | 455 | 120 | 0.4 | 0.7 | 0.32 | 9.8970 | 2.455 | -7.78332 |
| **5** | 455 | 180 | 0.6 | 0.9 | 0.38 | 8.4043 | 3.000 | -9.54243 |
| **6** | 455 | 240 | 0.8 | 0.5 | 0.41 | 7.7443 | 2.912 | -9.24796 |
| **7** | 783 | 120 | 0.6 | 0.5 | 0.42 | 7.5350 | 0.895 | 1.01220 |
| **8** | 783 | 180 | 0.8 | 0.7 | 0.43 | 7.3306 | 1.205 | -1.58362 |
| **9** | 783 | 240 | 0.4 | 0.9 | 0.45 | 6.9357 | 0.781 | 2.158108 |
| **10** | 836 | 120 | 0.8 | 0.9 | 0.50 | 6.0206 | 1.903 | -5.57507 |
| **11** | 836 | 180 | 0.4 | 0.5 | 0.47 | 6.5580 | 0.452 | 6.93575 |
| **12** | 836 | 240 | 0.6 | 0.7 | 0.48 | 6.3752 | 0.851 | 1.411621 |
| **13** | 417 | 120 | 0.6 | 0.9 | 0.30 | 10.4576 | 3.114 | -9.82723 |
| **14** | 417 | 180 | 0.8 | 0.5 | 0.31 | 10.1728 | 3.151 | -9.96621 |
| **15** | 417 | 240 | 0.4 | 0.7 | 0.35 | 9.1186 | 1.209 | -1.58362 |
| **16** | 442 | 120 | 0.8 | 0.7 | 0.32 | 9.8970 | 2.801 | -8.94316 |
| **17** | 442 | 180 | 0.4 | 0.9 | 0.34 | 9.3704 | 2.555 | -8.13080 |
| **18** | 442 | 240 | 0.6 | 0.5 | 0.35 | 9.1186 | 2.671 | -8.29947 |

The Taguchi S/N response table was used to analyze the effect of the input parameters on the output parameters (Vb and Ra). Table 5.3 shows the S/N response table showing the effect of each control factor on the output parameters. In Table 5.3, the largest S/N ratio indicates the control factors being at optimum levels and accordingly, the data indicate in bold in the table represent optimum levels for cutting parameters [93]. As can be deduced in Table 5.3, the ideal input parameters levels for the Vb were found to be Alloy I, a cutting depth is 0.5mm, the cutting speed is 120m/min and the feed rate is 0.4mm/tooth. With these parameters, the lower tool wear was measured as 0.28 mm in the machining of Alloy I. Similarly, the ideal input parameters for the Ra were specified as Alloy VIII, the depth of cut of 0.5 mm, the cutting speed of 240 m/min and the feed rate of 0.4 mm/tooth. With these parameters, the lower surface roughness was measured as 0.415 µm in the machining of Alloy VIII.

ANOVA was applied to investigate the effect of milling parameters on the tool wear and surface roughness. The results of ANOVA are shown in Table 5.4. In Table 5.4, the F values show the effect levels of the input parameters and the contribution rates

are defined by taking this parameter into account [94]. The parameter with the largest F value is the factor that has the greatest effect on the result [95,96]. As can be deduced in Table 5.4, the most important parameter affecting both tool wear and surface roughness is the workpiece material with an additive ratio of 89.1 and 72.85%, respectively. On the other hand, Pareto analysis was used to determine the significance of the input parameters on the output parameters (Vb and Ra). Pareto charts for the output parameters (Vb and Ra) are given in Figure 5.8. As is displayed in Figure 5.8, the most effective factor on both tool wear and surface roughness is the workpiece material.

Table 5.3. S/N response of experiment results.

| | **Cutting factors** | | | | | | | |
|---|---|---|---|---|---|---|---|---|
| | **A** | **B** | **C** | **D** | **A** | **B** | **C** | **D** |
| ***Vb*** | | | | | ***Ra*** | | | |
| **1** | **10.295** | **9.144** | **8.823** | **8.698** | -10.3573 | -6.5693 | **-2.7839** | **-4.6442** |
| **2** | 9.916 | 8.716 | 8.725 | 8.846 | -7.1257 | -5.3984 | -5.8914 | -4.7642 |
| **3** | 9.462 | 8.110 | 8.423 | 8.427 | -8.4578 | **-4.7051** | -7.9976 | -7.2645 |
| **4** | 8.682 | | | | -8.8579 | | | |
| **5** | 7.267 | | | | 0.5289 | | | |
| **6** | 6.318 | 1.034 | 0.400 | 0.419 | **0.9241** | | | |
| **Delta** | 3.977 | | | | 11.2814 | 1.8642 | 5.2137 | 2.6203 |

Table 5.4. Result of variance for the output parameters.

| **Factors** | **Degree of freedom (DoF)** | **Sum of squares (SS)** | **Mean square (MS)** | **F ratio** | **P ratio** | **Contribution rate (%)** |
|---|---|---|---|---|---|---|
| ***Vb*** | | | | | | |
| Ct | 5 | 0.072983 | 0.014597 | 43.79 | 0.000 | 89.17 |
| Vc (m/min) | 2 | 0.004900 | 0.002450 | 7.35 | 0.024 | 5.99 |
| f (mm/rev) | 2 | 0.000933 | 0.000467 | 1.40 | 0.317 | 1.14 |
| *a (mm)* | 2 | 0.001033 | 0.000517 | 1.55 | 0.287 | 1.26 |
| Error | 6 | 0.002000 | 0.000333 | | | 2.44 |
| Total | 17 | 0.081850 | | | | 100 |
| ***Ra*** | | | | | | |
| Ct | 5 | 14.4378 | 2.88756 | 29.03 | 0.000 | 72.85 |
| Vc (m/min) | 2 | 0.1175 | 0.05874 | 0.59 | 0.583 | 0.59 |
| *f* (mm/rev) | 2 | 3.2518 | 1.62591 | 16.35 | 0.004 | 16.41 |
| *a (mm)* | 2 | 1.4155 | 0.70774 | 7.12 | 0.026 | 7.14 |
| Error | 6 | 0.5968 | 0.09946 | | | 3.01 |
| Total | 17 | 19.8193 | | | | 100 |

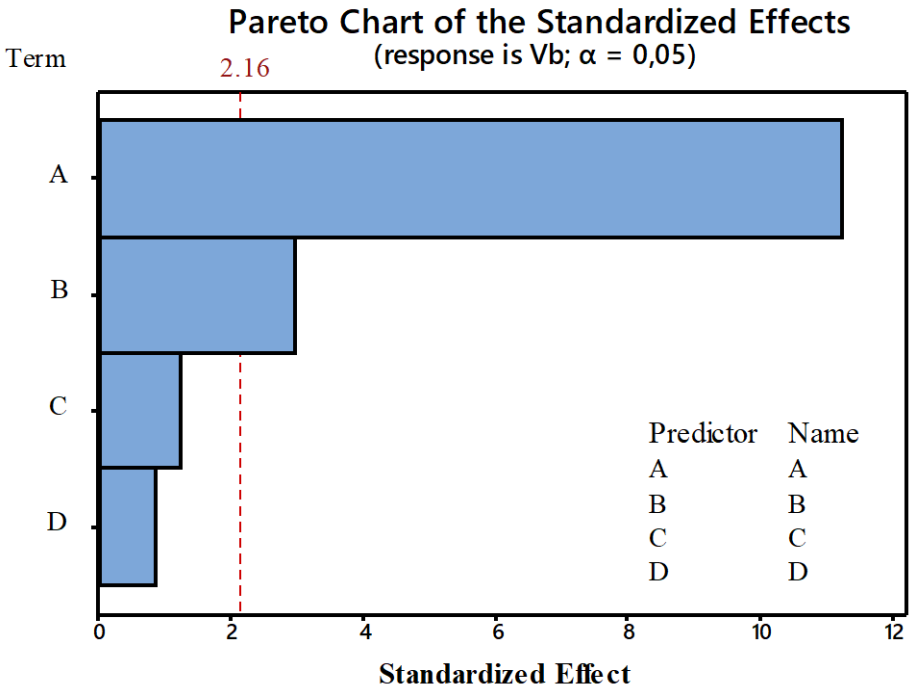


a)

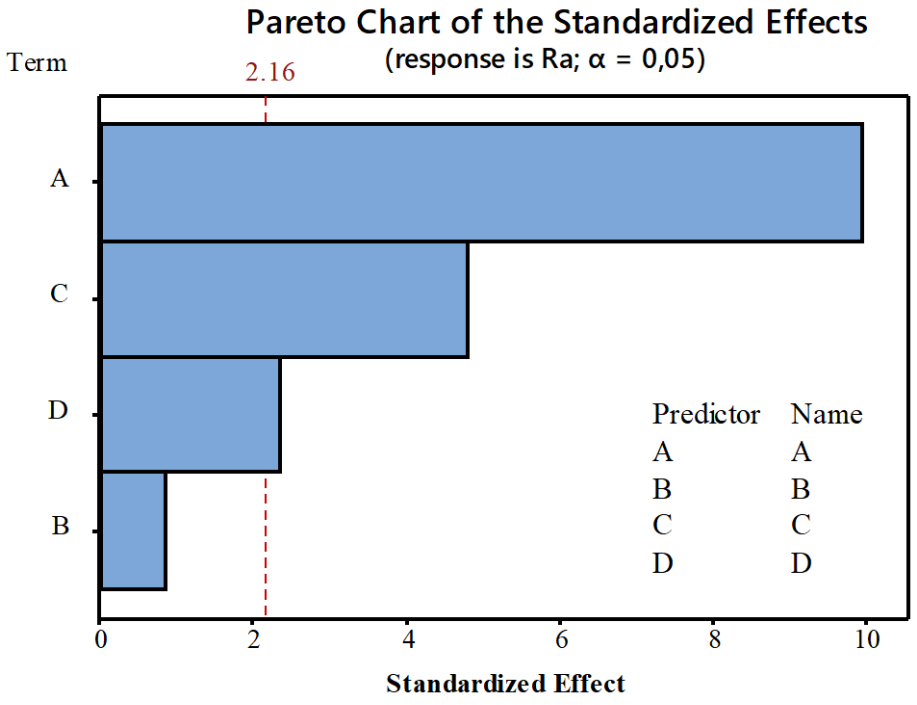


b)

Figure 5.8. Pareto charts for a) Vb and b) Ra.

## 5.5. MATHEMATICAL MODELING OF SURFACE ROUGHNESS AND TOOL WEAR

The correlations between input factors and output parameters (Vb and Ra) were expressed using linear and quadratic regressions. The final response equations derived for the output parameters (Vb and Ra) and determination coefficients are given in Table 5.5. Figure 5.9 also shows the comparison of experimental results and estimated values obtained by quadratic regression analysis for the output parameters (Vb and Ra).

Table 5.5. Developed equations for the output parameters.

| Factor | Equation | $R^2$ (%) |
|---|---|---|
| **Vb** | $Vb_I = 0.1022 + 0.000311Ct + 0.000333Vc + 0.0417f + 0.0292a$ | 91.38 |
| | $Vb_q = 0.204 + 0.000415Ct + 0.00081Vc - 0.291f - 0.168a - 0.0000001Ct^2 - 0.0000001Vc^2 + 0.032f^2 + 0.007a^2 - 0.000001Ct * Vc - 0.00007Ct * f + 0.000257Ct * a + 0.00077Vc * f - 0.00037Vc * a + 0.213f * a$ | 95.08 |
| **Ra** | $Ra_I = 2.434 - 0.00442Ct - 0.00154Vc + 2.592f + 1.267a$ | 90.81 |
| | $Ra_q = 3.15 - 0.00026Ct + 0.0067Vc + 2.08f - 5.3a - 0.000002Ct^2 - 0.000044Vc^2 - 3.75f^2 + 2.62a^2 - 0.000009Ct * Vc - 0.00647Ct * f + 0.00576Ct * a + 0.0303Vc * f - 0.01Vc * a + 3.52f * a$ | 98.95 |

As can be deduced in Table 5.5, the high ($R^2$) values of second-degree models compared to linear models indicate that second-degree models are more successful in estimating output parameters. Furthermore, as can be seen Figure 5.9, the experimental and estimated values are very close to each other.

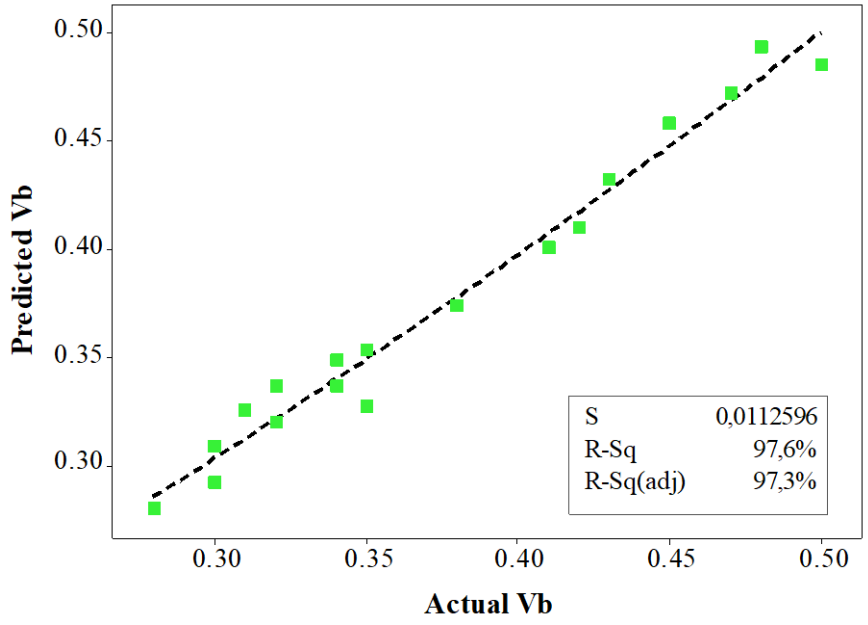


a)

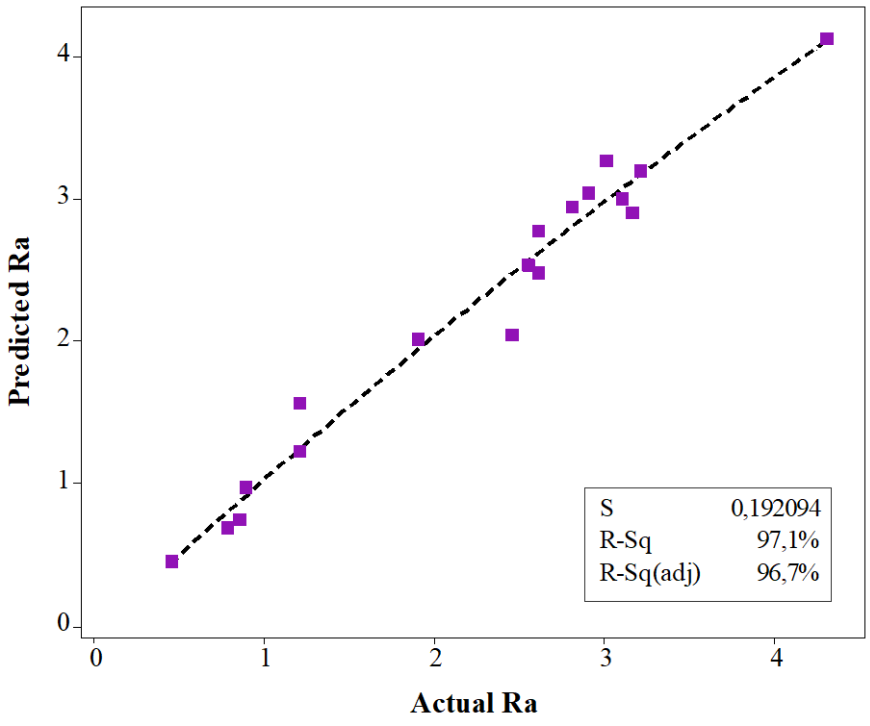


b)

Figure 5.9. The plot of actual and predicted values for (a) Vb, and (b) Ra.

## 5.6. VERIFICATION OF THE OPTIMIZATION PROCESS

The accuracy of the optimization process was tested by considering the confidence interval. In this context, the confidence intervals (CI) have been calculated by using Equations 5.1, 5.2. $F_{0.05,1,6} = 5.9874$ (From F test table), $Ve_{Vb} = 0.000333$ and $Ve_{Ra} = 0.09946$ (Table 5.3),$R = 1$, $N = 18$, $T_{dof} = 11$, and $n_{eff} = 1.5$ (Equation 5.1). $\mathrm{CI_{Vb}}$, and $\mathrm{CI_{Ra}}$ were calculated as 0.057 and 0.996 by using Equation (5.2), respectively.

$$n_{eff} = \frac{N}{1+T_{dof}} \tag{5.1}$$

$$CI_{Vb,Ra} = \sqrt{F_{a,1,fe}\, V_e \left[\frac{1}{n_{eff}} + \frac{1}{R}\right]} \tag{5.2}$$

As can be deduced from Table 5.2, the ideal level groups for the lowest Vb, and Ra values are A1B1C1D1, and A8B3C1D1, respectively. The estimated optimum values were calculated using the models shown in Equations 5.3-5.6, respectively.

$$Vb_{opt} = (A_1 - T_{Vb}) + (B_1 - T_{Vb}) + (C_1 - T_{Vb}) + (D_1 - T_{Vb}) + T_{Vb} \tag{5.3}$$

$$Ra_{opt} = (A_6 - T_{Ra}) + (B_3 - T_{Ra}) + (C_1 - T_{Ra}) + (D_1 - T_{Ra}) + T_{Ra} \tag{5.4}$$

$T_{Vb}$, and $T_{Ra}$ is the average of the values obtained in the experiments for each output parameter. $T_{Vb}$, and $T_{Ra}$ values are calculated to be 0.375 mm, and 2.217 µm, respectively. As a result of the calculations, $Vb_{opt}$, and $Ra_{opt}$ values are found to be 0.281 mm, and 0.294 µm, respectively.

$$\left[Vb_{opt} - CI_{Vb}\right] < Vb_{exp} < \left[FVb_{opt} + CI_{Vb}\right] = \tag{5.5}$$
$$[0.281 - 0.057] < 0.28 < [0.281 + 0.057] = 0.224 < 0.28 < 0.338$$

$$\left[Ra_{opt} - CI_{Ra}\right] < Ra_{exp} < \left[Ra_{opt} + CI_{Ra}\right] = \tag{5.6}$$
$$[0.294 - 0.996] < 0.395 < [0.294 + 0.996] = -0.702 < 0.415 < 1.29$$

The validation results indicate that the $Vb_{exp}\ and\ Ra_{exp}$values obtained at the optimum cutting parameters are within the confidence interval limits. Based on this situation, it can be concluded that the optimization process for the output parameters (Vb and Ra) was performed at a significance level of 0.05 using the Taguchi method [97,98].

## 5.7. CORROSION TEST RESULTS

After performing the corrosion tests and applying the parameters in Table 4.3 at 25 ºC, the results shown in Table 5.6 and Figure 5.10 were obtained.

Table 5.6. Corrosion test results.

| **Specimen** | **CCD ($\mu A / cm^2$)** | **CR (mm / year)** | **$E_{corr}$ (V)** |
|---|---|---|---|
| Fe-C | 58.66 | 0.475 | -0.59 |
| 3Cr5Mo | 26.25 | 0.218 | -0.35 |
| 316L | 0.943 | 0.008 | -0.17 |

In Table 5.6 CCD refers to Corrosion Current Density ($i_{corr}$), CR: Corrosion Rate and $E_{corr}$: Corrosion Potential [99,100].

Equivalent Weight (EW) can be defined as the mass of metal in grams that will be oxidized by the passage of one Faraday (96,489 ± 2 C (coulombs)) of electric charge. To calculate the equivalent weight of an alloy, Equation 5.7 can be used [99,100]:

$$EW = \frac{1}{\sum \frac{nifi}{Wi}} \tag{5.7}$$

Where ni: the valence of the $i^{th}$ element of the alloy, fi: the mass fraction of the $i^{th}$ element in the alloy and Wi: the atomic weight of the $i^{th}$ element in the alloy.

Faraday's Law in Equation 5.8 can be used to calculate the corrosion rate (CR) of samples [101].

$$CR = \frac{\lambda \times i_{corr}}{\mathrm{d}} \times EW \tag{5.8}$$

Where $\lambda = 3.27\times10^{-3}$ (mm. g)/ (mA. cm. year), and d is density in g/cm$^3$ [101].

The polarization curves of the samples are shown in Figure 5.10.

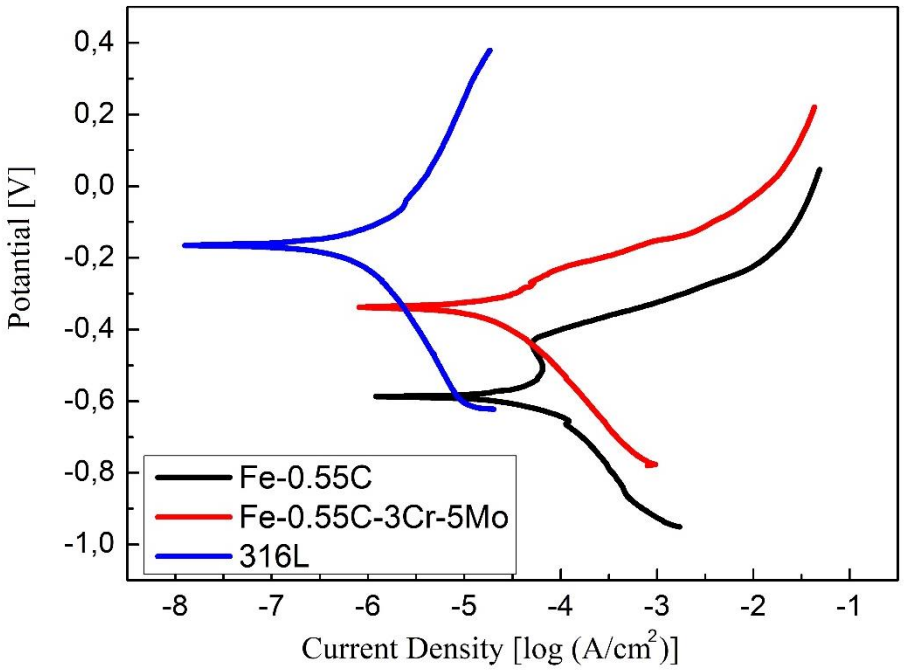


Figure 5.10. Polarization curves of the samples.

From the Table 5.6 and Figure 5.10, it is clear that the sample 316L has the highest corrosion resistance (the lowest corrosion rate). It is reported that the corrosion rate of 316L is 0.008 mm/year.

The sample containing only iron and carbon shows less resistance to corrosion than the rest of the samples, while the percentage of corrosion resistance increased after adding chromium and molybdenum to the alloy.

The corrosion resistance of the PM sample containing 3Cr-5Mo - which had the highest mechanical properties - was higher than the non-alloyed steel without Cr-Mo added.

The corrosion rate of the PM sample containing 3Cr5Mo was 0.218 mm/year, while the corrosion rate of the unalloyed steel was 0.475 mm/year, which means that the sample containing Cr-Mo has twice the corrosion resistance.

Although samples containing Cr-Mo have a much greater corrosion resistance than non-alloyed steel samples, the corrosion rate is relatively high if we want to use this metal in medical implant applications, which means that it cannot be used directly in the manufacture of medical implants [48].

Alloys containing Cr-Mo have significantly higher hardness and tensile strength than 316L stainless steels. Which gives it an advantage in terms of mechanical properties, and it can be a good solution in the field of manufacturing medical implants only if a solution to the problem of high corrosion rate is found.

## 5.8. CONCLUSION

In this study, Fe-C steels containing different proportions of Cr and Mo were produced using the powder metallurgy method. The mechanical properties were characterized in terms of tensile and yield strengths, % elongation values and hardness values considering the microstructure images. Then, the machining tests were performed using a CNC machine with different cutting parameters. The data obtained in the milling tests were also analyzed statistically. The important and main findings of this study are summarized below:

- When molybdenum and chromium alloying elements were added to the composite, the pearlite ratio in the steel produced using the powder metallurgy method was increased.

- EDS analyzes of PM steels reveal that the elements Mo, C and N and the precipitates formed by these elements such as MoC(N), CrC(N) and CrMoC(N) are present in the iron matrix composite.

- The tensile test results showed that the yield strength, and tensile strength increased, but the elongation ratio values decreased with the increase of Mo content up to a certain level, and also that the mechanical properties of steels with alloyed elements are superior to those without alloying elements.

- The output parameters (Fc, Ra, and Vb) increased depending on the increasing feed rate.

- The Taguchi analysis showed that the ideal level groups for the lowest Vb, and Ra were A1B1C1D1, and A8B3C1D1, respectively.

- The lowest Vb value was obtained as 0.152 mm in the milling of the Alloy I sample at 0.4 mm/tooth feed rate and 150 m/min cutting speed.

- The lowest surface roughness value was measured as 0.38 μm in the milling of the Alloy IV sample at 0.4 mm/tooth feed rate and 270 m/min cutting speed.

- SEM investigation revealed that the flank wear and nose wear were observed as the dominant wear modes for all the cutting tools.

- The most effective factor on both tool wear and surface roughness is the workpiece material according to the results of analysis of variance.

- First and second-order models developed to estimate the output parameters (Vb, and Ra) give successful results with high coefficients of determination ($R^2$).

- When the corrosion results are examined, the highest corrosion resistance was observed in 316L material, while the lowest corrosion resistance was observed in the unalloyed steel sample.

- Although samples containing Cr-Mo have higher tensile strength and hardness, good mechanical properties and relatively good corrosion resistance, their use in the field of medical implants is limited because of the relatively high corrosion rate for use in medical implants in the human body.

## REFERENCES


1. Sukhanov, D. A., Plotnikova, N. V., Sukhanov, D. A., and Plotnikova, N. V., "Wootz: Cast Iron or Steel?", ***Materials Sciences And Applications***, 7 (11): 792–802 (2016).

2. Internet: Föll, H., "Overview of Major Steels", **https://www.tf.uni-kiel.de/matwis/amat/iss/kap_9/advanced/t9_2_1b.html** (2021).

3. Arthur, D. E., Jonathan, A., Ameh, P. O., and Anya, C., "A review on the assessment of polymeric materials used as corrosion inhibitor of metals and alloys", ***International Journal Of Industrial Chemistry 2013 4:1***, 4 (1): 1–9 (2013).

4. Edmonds, D. V, He, K., Rizzo, F. C., De Cooman, B. C., Matlock, D. K., and Speer, J. G., "Quenching and partitioning martensite—A novel steel heat treatment", ***Materials Science And Engineering: A***, 438: 25–34 (2006).

5. Bramfitt, B. L. and Benscoter, A. O., "Metallographer's Guide: Practice and Procedures for Irons and Steels", ***Asm International***, (2001).

6. Vitos, L., Zhang, H. L., Lu, S., Al-Zoubi, N., Johansson, B., Nurmi, E., Ropo, M., J. Punkkinen, M. P., and Kokko, K., "Alloy Steel: Properties and Use First-Principles Quantum Mechanical Approach to Stainless Steel Alloys", ***Alloy Steel - Properties And Use***, (2011).

7. KÖKSAL, Ü., "The effect of sintering time on mechanical characteristics of Ni-Mo steel added W-Nb-V produced with powder metallurgy", Master thesis, ***University of Karabük Department of Manufacturing Engineering***, Karabük, (2021).

8. Zhou, W., Northwood, D. O., and Liu, C., "A steel-like unalloyed multiphase ductile iron", ***Journal Of Materials Research And Technology***, 15: 3836–3849 (2021).

9. Tekin, E., "Mühendisler Için Çelik Seçimi", ***TMMOB Makina Mühendisleri Odası***, (1992).

10. Rao, P. N., "Manufacturing Technology: Foundry, Forming and Welding", 5. Ed., ***McGraw-Hill Education***, Cedar Falls, (2018).

11. Natesan, E., Eriksson, S., Ahlström, J., and Persson, C., "Effect of temperature on deformation and fatigue behaviour of A356–T7 cast aluminium alloys used in high specific power IC engine cylinder heads", ***Materials***, 13 (5): 1202 (2020).

12. Hummel, R. E., "Understanding Materials Science: History, Properties, Applications, Second Edition", ***Springer***, (2004).

13. Erden, M. A., "The effect of the sintering temperature and addition of niobium and vanadium on the microstructure and mechanical properties of microalloyed PM steels", ***Metals***, 7 (9): 329 (2017).

14. Erden, M. A. and Aydın, F., "Wear and mechanical properties of carburized AISI 8620 steel produced by powder metallurgy", ***International Journal Of Minerals, Metallurgy And Materials 2021 28:3***, 28 (3): 430–439 (2021).

15. Karabulut, H., Türkmen, M., Erden, M. A., and Gündüz, S., "Effect of Different Current Values on Microstructure and Mechanical Properties of Microalloyed Steels Joined by the Submerged Arc Welding Method", ***Metals 2016, Vol. 6, Page 281***, 6 (11): 281 (2016).

16. Gündüz, S., Karabulut, H., Erden, M. A., and Türkmen, M., "Microstructural effects on fatigue behaviour of a forged medium carbon microalloyed steel", ***Materials Testing***, 55 (11–12): 865–870 (2013).

17. Türkmen, M., Erden, M. A., Karabulut, H., and Gündüz, S., "The effects of heat treatment on the microstructure and mechanical properties of Nb–V microalloyed powder metallurgy steels", ***Acta Phys. Pol. A***, 135: 834–836 (2019).

18. ERDEN, M., GÜNDÜZ, S., ÇALIGÜLÜ, U., and Boz, M., "Investigation of hardness and microstructure properties of non alloyed and hardox steel combined with submerged arc welding method", (2018).

19. Türkmen, M., Karabulut, H., Erden, M. A., and Gündüz, S., "Effect of TiN addition on The microstructure and mechanical properties of PM steels", ***Technological Applied Sciences***, 12 (4): 178–184 (2017).

20. Simsir, H., Akgul, Y., and Erden, M. A., "Hydrothermal carbon effect on iron matrix composites produced by powder metallurgy", ***Materials Chemistry And Physics***, 242: 122557 (2020).

21. Ahssi, M. A. M., Erden, M. A., Acarer, M., and Çuğ, H., "The Effect of Nickel on the Microstructure, Mechanical Properties and Corrosion Properties of Niobium–Vanadium Microalloyed Powder Metallurgy Steels", ***Materials***, 13 (18): 4021 (2020).

22. Muhamed, G. A., Gündüz, S., Erden, M. A., and Taştemur, D., "Dynamic Strain Aging behaviour in AISI 316L austenitic stainless steel under as-received and as-welded conditions", ***Metals***, 7 (9): 362 (2017).

23. Kim, N. J., "The Physical Metallurgy of HSLA Linepipe Steels—A Review", ***JOM***, 35 (4): 21–27 (1983).

24. Taş, Z., "Yüksek dayanımlı düşük alaşımlı çeliklerde metalürjik mukavemet artırma mekanizmaları", ***Erciyes Üniversitesi Fen Bilimleri Enstitüsü Fen Bilimleri Dergisi***, 28 (2): 97–101 (2012).

25. Pierson, H. O., "Handbook of Carbon, Graphite, Diamonds and Fullerenes: Processing, Properties and Applications", ***William Andrew***, (2012).

26. Karabulut, H., "The effect of strain ageing on the mechanical properties of microalloyed steels", Master Thesis, ***Zonguldak Bülent Ecevit University, Graduate School of Natural and Applied Sciences***, Zonguldak, (2004).

27. Loos, M., "Allotropes of Carbon and Carbon Nanotubes", Carbon Nanotube Reinforced Composites: CNR Polymer Science and Technology, 73–101 (2015).

28. Internet: Popova, M., "The Surprising History of the Pencil ", **https://www.themarginalian.org/2013/06/24/history-of-the-pencil/** (2021).

29. Burchell, T. D., "Carbon Materials for Advanced Technologies", ***Elsevier Science***, (1999).

30. Mokhena, T. C., Mochane, M. J., Sefadi, J. S., Motloung, S. V., and Andala, D. M., "Thermal Conductivity of Graphite-Based Polymer Composites", ***Impact Of Thermal Conductivity On Energy Technologies***, (2018).

31. Speight, J. G., "Handbook of Petroleum Product Analysis", ***John Wiley & Sons***, (2015).

32. Topbaş, M. A., "Çelik Isıl Işlem El Kitabı", 1. Ed., ***PRESTİJ YAYINCILIK***, Istanbul, (1998).

33. Dokumacı, E. and Önay, B., "Oxidation behavior of Mo containing alloys", ***Materials Science Forum***, 595: 959–966 (2008).

34. Internet: Çetin, A., "Çeliklerde Alaşım Elementlerinin Etkileri", **https://dokumhane.net/kutuphane/celiklerde-alasim-elementlerinin-etkileri/** (2021).

35. Šalak, A., Selecká, M., and Danninger, H., "Machinability of Powder Metallurgy Steels", ***Cambridge Int Science Publishing***, (2005).

36. Narasimhan, K. S. and Semel, F. J., "Sintering of powder premixes-a brief overview", ***Advances In Powder Metallurgy And Particulate Materials***, 1 (05): (2007).

37. Aşkun, Y., HASIRCI, H., and ŞEKER, U., "Ni VE Cu İLE ALAŞIMLANDIRILMIŞ KÜRESEL GRAFİTLİDÖKME DEMİRLERİN İŞLENEBİLİRLİĞİNİN KESME KUVVETLERİ VE YÜZEY KALİTELERİ AÇISINDAN DEĞERLENDİRİLMESİ", ***Pamukkale University Journal Of***

***Engineering Sciences***, 9 (2): 191–199 (2003).

38. Genchi, G., Carocci, A., Lauria, G., Sinicropi, M. S., and Catalano, A., "Nickel: Human Health and Environmental Toxicology", ***International Journal Of Environmental Research And Public Health***, 17 (3): (2020).

39. Cadosch, D., Chan, E., Gautschi, O. P., and Filgueira, L., "Metal is not inert: Role of metal ions released by biocorrosion in aseptic loosening—Current concepts", ***Journal Of Biomedical Materials Research Part A***, 91A (4): 1252–1262 (2009).

40. Manivasagam, G., Dhinasekaran, D., and Rajamanickam, A., "Biomedical Implants: Corrosion and its Prevention - A Review", ***Recent Patents On Corrosion Science***, 2 (1): 40–54 (2010).

41. Urish, K., Anderson, P., Mihalko, W., and Committee, A. B. E., "The challenge of corrosion in orthopaedic implants", ***AAOS Now. April***, (2013).

42. Almasry, M. G., "CORROSION BEHAVIOR OF ORTHOPEDIC IMPLANTS IN THE PATIENT BODY AND ITS DEBRİS", Master thesis, ***Erciyes University***, Kayseri, (2021).

43. Dexter, S. C., "Galvanic Corrosion", ***Niversity Of Delaware Sea Grant College Program***, (1999).

44. Internet: Aydın, T., "Galvanic Series Noble Metals.Jpg", **https://tr.m.wikipedia.org/wiki/Dosya:Galvanic_series_noble_metals.jpg** (2022).

45. Chen, Q. and Thouas, G., "Biomaterials: A Basic Introduction", ***CRC Press***, (2014).

46. Landolt, D. and Mischler, S., "Tribocorrosion of Passive Metals and Coatings", ***Elsevier***, (2011).

47. dos Santos, C. T., Barbosa, C., Monteiro, M. de J., Abud, I. de C., Caminha, I. M. V., and Roesler, C. R. de M., "Fretting corrosion tests on orthopedic plates and screws made of ASTM F138 stainless steel", ***Research On Biomedical Engineering***, 31 (2): 169–175 (2015).

48. Eliaz, N., "Corrosion of Metallic Biomaterials: A Review", ***Materials***, 12 (3): 407 (2019).

49. Kamachi Mudali, U., Sridhar, T. M., and Baldev, R. A. J., "Corrosion of bio implants", ***Sadhana***, 28 (3): 601–637 (2003).

50. Gilbert, J. L., "Corrosion in the Human Body: Metallic Implants in the Complex Body Environment", ***Corrosion***, 73 (12): 1478–1495 (2017).

51. Internet: DDCoating, "What Is Pitting Corrosion? How to Detect and Treat Pitting Corrosion?", **https://www.ddcoatings.co.uk/2276/what-is-pitting-corrosion** (2022).

52. Panda, A., Dobransky, J., Jančík, M., Pandova, I., and Kačalová, M., "Advantages and effectiveness of the powder metallurgy in manufacturing technologies", ***Metalurgija***, 57 (4): 353–356 (2018).

53. Söyler, M., "Powder metallurgy and applications", Master Thesis, ***Gebze Institute of Technology***, Gebze, (2007).

54. Tripathy, A., Sarangi, S. K., and Chaubey, A. K., "A review of solid state processes in manufacture of functionally graded materials", ***Int. J. Eng. Technol***, 7: 1–5 (2018).

55. Dogan, C. and Saritas, S., "METAL-POWDER PRODUCTION BY CENTRIFUGAL ATOMIZATION", (1994).

56. Internet: Metal Powder Industries Federation, "Making Metal Powder", **https://www.mpif.org/IntrotoPM/MakingMetalPowder.aspx** (2021).

57. Internet: SubsTech, "Powder Preparation ", **https://www.substech.com/dokuwiki/doku.php?id=powder_preparation** (2021).

58. Beddow, J. K., "Production of Metal powders by atomization", ***Heyden And Son Inc., Philadelphia, Pa. 1978, 100 P***, (1978).

59. Ersümer, A., "Toz Metallürjisi: Sert Metal, Sinterleme", ***Istanbul Technical University Library***, (1970).

60. German, R., "Powder Metallurgy Science" second edition, metal powder industries federation", (1994).

61. Mirski, Z., Pabian, J., Wojdat, T., and Hejna, J., "Significance of the brazing gap in the brazing of aluminium heat exchangers for automotive industry", ***Welding Technology Review***, 92 (4): 7–14 (2020).

62. Internet: ÜNAL, R., "Toz Üretimi", **https://rahmiunal.net/toz/tozuretimi/powder_product.html** (2021).

63. Nakajima, Y., Yamamoto, J., Kanada, S., Masanobu, S., Takahashi, I., Okaya, K., Matsuo, S., Fukushima, T., and Fujita, T., "Study on grinding technology for seafloor mineral processing", ***Proceedings Of The International Conference On Offshore Mechanics And Arctic Engineering - OMAE***, 3: (2013).

64. Internet: Allen, E., "Ball Mill- Highly Efficient Grinding And Milling Machine", **https://www.everysingletopic.com/ball-mill-highly-efficient-grinding-and-milling-machine/** (2021).

65. Sarıtaş, S., Türker, M., and Durlu, N., "Toz metalurjisi ve parçacıklı malzeme işlemleri", ***Türk Toz Metalurjisi Yayınları***, 5: 2–34 (2007).

66. Alonso, M., Kousaka, Y., Hashimoto, T., and Hashimoto, N., "Penetration of nanometer-sized aerosol particles through wire screen and laminar flow tube", ***Aerosol Science And Technology***, 27 (4): 471–480 (1997).

67. German, R. M., "Powder Metallurgy and Particulate Materials Processing: The Processes, Materials, Products, Properties and Applications", ***Metal Powder Industries Federation***, (2005).

68. Onur, A., "Yağ Atomizasyonu Yöntemiyle Metal Tozu Üretiminin İncelenmesi", Master thesis, ***Karadeniz Technical University Institute of Natural and Applied Sciences***, Trabzon, (1996).

69. Internet: Russo, M., "Understanding the Powdered Metal Process: Spotlight on Compacting", **https://www.nationalbronze.com/News/understanding-the-powdered-metal-process-spotlight-on-compacting/** (2022).

70. Internet: Dalton, D., "METAL POWDER PROCESSING TECHNIQUES", **https://slideplayer.com/slide/7362890/** (2021).

71. HİÇYILMAZ, N., "Wear behaviour ceramic reinforced aluminum-base particulate composites produced by powder metallurgy", Master Thesis, ***Gazi University, Graduate School of Natural and Applied Sciences***, Ankara, (1999).

72. Erden, M. A., "An investigation on the relation sheep between microstructure and mechanical properties of microalloyed steels produced by powder metallurgy", Phd. Thesis, ***Karabuk University Department of Metallurgical Engineering***, Karabuk, (2015).

73. Internet: Open University, "Cold Isostatic Pressing - OpenLearn", **https://www.open.edu/openlearn/science-maths-technology/engineering-technology/manupedia/cold-isostatic-pressing** (2022).

74. Ageev, S. V. and Girshov, V. L., "Hot Isostatic Pressing of Metal Powders", ***Metallurgist***, 59 (7–8): 647–652 (2015).

75. AKGÜN, M., "Experimental numerical and statistical investigation of the effect of cryogenic treatment applied on cutting tools on machinability of inconel 625 nickel based superalloy", PhD Thesis, ***University of Karabuk Department of Manufacturing Engineering***, Karabük, (2021).

76. Zhu, Y., "Processing of Metallic Materials Lecture Notes", ***NC State University Department of Material Science and Engineering***, Karabuk, .

77. Internet: International Organization for Standardization, "ISO 8688-2, Tool Life Testing in Milling, Part 2: End Milling", **https://www.iso.org/standard/16092.html** .

78. Internet: oscarcot, "Three Electrode Measurement for AD5933", **https://ez.analog.com/data_converters/precision_dacs/f/q-a/27161/three-electrode-measurement-for-ad5933** (2022).

79. Internet: Princeton applied research, "PARSTAT 4000 Potentiostat/Galvanostat/EIS Analyzer", **https://www.gammadata.se/assets/Uploads/PARSTAT-4000-A4.pdf** (2022).

80. Erden, M. A., Yaşar, N., Korkmaz, M. E., Ayvacı, B., Ross, K. N. S., and Mia, M., "Investigation of microstructure, mechanical and machinability properties of Mo-added steel produced by powder metallurgy method", ***The International Journal Of Advanced Manufacturing Technology***, 114 (9): 2811–2827 (2021).

81. Özdemirler, D., Gündüz, S., and Erden, M. A., "Influence of NbC addition on the sintering behaviour of medium carbon PM steels", ***Metals***, 7 (4): 121 (2017).

82. Junhua, K., Lin, Z., Bin, G., Pinghe, L., Aihua, W., and Changsheng, X., "Influence of Mo content on microstructure and mechanical properties of high strength pipeline steel", ***Materials & Design***, 25 (8): 723–728 (2004).

83. Lee, W. B., Hong, S. G., Park, C. G., Kim, K. H., and Park, S. H., "Influence of Mo on precipitation hardening in hot rolled HSLA steels containing Nb", ***Scripta Materialia***, 43 (4): 319–324 (2000).

84. Erden, M. A., Gündüz, S., Karabulut, H., and Türkmen, M., "Wear behaviour of sintered steels obtained using powder metallurgy method", ***Mechanika***, 23 (4): 574–580 (2017).

85. Korchynsky, M., "Microalloying and thermo-mechanical treatment", ***16 Th Metals Congress Of The GDR: Thermomechanical Treatment Of Steel.***, 1: 96–137 (1987).

86. Kostryzhev, A. G., Al Shahrani, A., Zhu, C., Cairney, J. M., Ringer, S. P., Killmore, C. R., and Pereloma, E. V, "Effect of niobium clustering and precipitation on strength of an NbTi-microalloyed ferritic steel", ***Materials Science And Engineering: A***, 607: 226–235 (2014).

87. Gunduz, S., Erden, M. A., Karabulut, H., and Turkmen, M., "The effect of vanadium and titanium on mechanical properties of microalloyed PM steel", ***Powder Metallurgy And Metal Ceramics***, 55 (5): 277–287 (2016).

88. Erden, M. A., "Effect of C content on microstructure and mechanical properties of Nb-V added microalloyed steel produced by powder metallurgy method",

***Avrupa Bilim Ve Teknoloji Dergisi***, 5 (9): 44–47 (2016).

89. Shanmugasundaram, D. and Chandramouli, R., "Tensile and impact behaviour of sinter-forged Cr, Ni and Mo alloyed powder metallurgy steels", ***Materials & Design***, 30 (9): 3444–3449 (2009).

90. Ezugwu, E. O., Wang, Z. M., and Okeke, C. I., "Tool life and surface integrity when machining Inconel 718 with PVD-and CVD-coated tools", ***Tribology Transactions***, 42 (2): 353–360 (1999).

91. Ginting, A., Skein, R., Cuaca, D., and Masyithah, Z., "The characteristics of CVD-and PVD-coated carbide tools in hard turning of AISI 4340", ***Measurement***, 129: 548–557 (2018).

92. Bagherzadeh, A., Kuram, E., and Budak, E., "Experimental evaluation of eco-friendly hybrid cooling methods in slot milling of titanium alloy", ***Journal Of Cleaner Production***, 289: 125817 (2021).

93. Kıvak, T., "Optimization of surface roughness and flank wear using the Taguchi method in milling of Hadfield steel with PVD and CVD coated inserts", ***Measurement***, 50: 19–28 (2014).

94. Akgün, M. and Demir, H., "Estimation of surface roughness and flank wear in milling of Inconel 625 Superalloy", ***Surface Review And Letters***, 28 (04): 2150011 (2021).

95. Akgün, M. and Demir, H., "Optimization of Cutting Parameters Affecting Surface Roughness in Turning of Inconel 625 Superalloy by Cryogenically Treated Tungsten Carbide Inserts", ***SN Applied Sciences***, 3 (2): 1–12 (2021).

96. Özlü, B., "Experimental and statistical investigation of the effects of cutting parameters on kerf quality and surface roughness in laser cutting of Al 5083 alloy", ***Surface Review And Letters***, 28 (10): 2150093 (2021).

97. Cetin, M. H., Ozcelik, B., Kuram, E., and Demirbas, E., "Evaluation of vegetable based cutting fluids with extreme pressure and cutting parameters in turning of AISI 304L by Taguchi method", ***Journal Of Cleaner Production***, 19 (17–18): 2049–2056 (2011).

98. Kara, F. and Öztürk, B., "Comparison and optimization of PVD and CVD method on surface roughness and flank wear in hard-machining of DIN 1.2738 mold steel", ***Sensor Review***, (2018).

99. ASTM International, "Standard Practice for Calculation of Corrosion Rates and Related Information from Electrochemical Measurements", ***ASTM International***, (2010).

100. Turan, M. E. and Aydin, F., "Wear and corrosion properties of low-cost eggshell-reinforced green AZ91 matrix composites", ***Canadian Metallurgical Quarterly***, 61 (2): 155–171 (2022).

101. Demirdal, S. and Aydın, F., "The influence of low-cost eggshell on the wear and electrochemical corrosion behaviour of novel pure Mg matrix composites", ***Materials Chemistry And Physics***, 277: 125520 (2022).

## RESUME

Abdul Rahman VASSOUF had completed his elementary, middle and high school in Hail city – Saudi Arabia. After that he joined the University of Karabuk as a student in Biomedical Engineering department in 2015, and graduated in 2020 with honor degree. In the same year, he began his postgraduate studies at Karabuk University as a master's student in the department of Biomedical Engineering.